São Paulo State University
School of Engineering, Bauru

Identification of damage in one-dimensional periodic structures

Luiza Ragoni Maniero

July, 2021

Luiza Ragoni Maniero

Identification of damage in one-dimensional periodic structures

A dissertation presented for the degree of Master
of Science at the São Paulo State University in a
partial fulfillment of the requirements.
Supervisor: Prof. Dr. Paulo José Paupitz Gonçalves

July, 2021

M278i

Maniero, Luiza Ragoni
Identification of damage in one-dimensional periodic structures / Luiza Ragoni Maniero. -- Bauru, 2021
62 p. : il., tabs., fotos

Dissertação (mestrado) - Universidade Estadual Paulista (Unesp), Faculdade de Engenharia, Bauru
Orientadora: Paulo José Paupitz Gonçalves

1. Structural Health Monitoring. 2. Periodic structure. 3. Identification of damage. I. Título.

Sistema de geração automática de fichas catalográficas da Unesp. Biblioteca da Faculdade de Engenharia, Bauru. Dados fornecidos pelo autor(a).

Essa ficha não pode ser modificada.

UNIVERSIDADE ESTADUAL PAULISTA

Câmpus de Bauru

ATA DA DEFESA PÚBLICA DA DISSERTAÇÃO DE MESTRADO DE LUIZA RAGONI MANIERO, DISCENTE DO PROGRAMA DE PÓS-GRADUAÇÃO EM ENGENHARIA MECÂNICA, DA FACULDADE DE ENGENHARIA - CÂMPUS DE BAURU.

Aos 06 dias do mês de agosto do ano de 2021, às 08:30 horas, por meio de Videoconferência, realizou-se a defesa de DISSERTAÇÃO DE MESTRADO de LUIZA RAGONI MANIERO, intitulada **IDENTIFICATION OF DAMAGE IN ONE-DIMENSIONAL PERIODIC STRUCTURES**. A Comissão Examinadora foi constituida pelos seguintes membros: Prof. Dr. PAULO JOSÉ PAUPITZ GONÇALVES (Orientador(a) - Participação Virtual) do(a) Departamento de Engenharia Mecânica / Faculdade de Engenharia de Bauru - UNESP, Prof. Dr. FABRICIO CESAR LOBATO DE ALMEIDA (Participação Virtual) do(a) Departamento de Engenharia de Biossistemas / Faculdade de Ciências e Engenharia de Tupã - UNESP, Prof. Dr. FERNANDO DE HARO MORAES (Participação Virtual) do(a) Departamento de Indústria / Instituto Federal de Educação, Ciência e Tecnologia de São Paulo, Campus Araraquara. Após a exposição pela mestranda e arguição pelos membros da Comissão Examinadora que participaram do ato, de forma presencial e/ou virtual, a discente recebeu o conceito final: APROVADA. Nada mais havendo, foi lavrada a presente ata, que após lida e aprovada, foi assinada pelo(a) Presidente(a) da Comissão Examinadora.

Prof. Dr. PAULO JOSÉ PAUPITZ GONÇALVES

I hereby declare that this thesis has been composed by myself and it has not been submitted for any previous application for a degree. All the work described in this thesis has been done by myself and all the sources of information have been specifically referenced.

Identification of damage in one-dimensional periodic structures

Luiza Ragoni Maniero

Keywords: structural health monitoring, periodic structure, identification of damage.

Abstract Periodic structures are generally found in many engineering applications. These structures generally consist of equal or similar sub-parts, which are assembled repetitively. Examples of periodic structures can be found on aircraft, buildings, bridges, train tracks, for example. For dynamic analysis, these structures have characteristics distinct from other structures, such as the formation of "band gaps", which are frequency bands where there is no wave propagation in the structure, or where the propagation is attenuated. Knowing that many of these structures may be subject to critical operating conditions, where there is a risk of failure, it is important to identify methods for monitoring structural health conditions. In this context, this work aims to develop an analysis based on frequency response metrics to identify changes in the structural dynamic behavior in one-dimensional systems such as bars and beams.The spectral element method simulated the conditions of structural damage, where the magnitude and location are changed. With the frequency response of each variation of the damage in the structure, correlation methods used: Frequency Response Curvature Method (FRF) and the Frequency Response Assurance Criterion (FRAC) to identify these characteristics. And for this simulation, a periodic structure with 10 cells with one and two damages was chosen, varying the damage from 2% to 30% and its position. The results of the two methods are complementary. The FRF Method localizes and quantifies the damage in the structure, except in the extremities due to the mathematical arrangement, and with the FRAC Method, it is possible to locate the damage in the extremities.

Identification of damage in one-dimensional periodic structures

Luiza Ragoni Maniero

Keywords: monitoramento da saúde estrutural, estrutura periódica, identificação de dano.

Abstract Estruturas periódicas são geralmente encontradas em diversas apliações de engenharia. Estas estruturas são geralmente constituídas de sub-partes iguais ou similares, que são montadas de forma repetitiva. Exemplos de estruturas periódicas podem ser encontrados em aeronaves, edifícios, pontes, trilhos de trem, por exemplo. Do ponto de vista da análise dinâmica, estas estruturas apresentam características distintas de outras estruturas, como por exemplo a formação de "band gaps", que são faixas de frequência em que não ocorre propagação de ondas na estrutura, ou em que a propagação ocorre de maneira atenuada. Tendo em vista que muitas destas estruturas podem estar sujeitas a condições de operação críticas, onde existe o risco de falhas, é importante identificar métodos de monitoramento da condições de saúde estutural. Neste contexto, este trabalho tem como objetivo desenvolver uma análise baseada em métricas de resposta em frequência para identificar alterações do comportamento dinâmico estrutural em sistemas unidimensionais como barras e vigas. O método de elementos espectrais foi utilizado para simular as condições do dano estrutural, modificando a sua magnitude e localização. Tendo a resposta em frequência de cada variação do dano na estrutura usou-se métodos de correlação: Método de Curvatura da Resposta em Frequência (FRF) e o Critério de garantia da resposta em frequência (FRAC) para identificar essas características. E para essa simulação escolheu-se uma estrutura periódica com 10 células com um e dois danos, variando o dano em 2% a 30% e sua posição. Os resultados dos dois métodos se complementam. O Método de FRF localica e quantifica o dano na estrutura, exceto nas extremidades devido ao arranjo matemático, e com o Método de FRAC é possível localizar o dano nas extremidade.

Acknowledgements

I would like to thank God, for letting me through all the difficulties. I have experienced your guidance day by day. You are the one who let me finish my degree. I will keep on trusting you for my future.

I would like to acknowledge and give my thanks to my supervisor Prof. Dr. Paulo José Paupitz Gonçalveswho made this work possible. His guidance and advice carried me through all the stages of writing my project. I would also like to thank the committee members Prof. Dr. Fabrício C L de Almeida and Prof. Dr. Fernando de Haro Moraes for your comments and suggestions to improve this dissertation. I wish to thank my fellow labmates. In special, my roommate Gabi for all these years sharing the academic life, home and friendship. I am also grateful to CAPES (process number: 88882.461711/2019-01) for the financial support.

I would also like to give special thanks to my family. My dear dad, my mom and my sister as a whole for their continuous support and understanding when undertaking my research and writing my project. Your prayer for me was what sustained me this far.

Agradeço ao meu pai, José Orlando, por ser para sempre o meu maior exemplo de amor, força e caráter. À minha mãe, Cláudia, agradeço por estar sempre ao meu lado e por ser minha inspiração. E à minha irmã, Carolina, obrigada por ser minha grande companheira da vida. Amor eterno por vocês.

Contents

List of Tables

List of Figures

Nomenclature

Designation	Explanation
Latin symbols	
A	cross section area
A_D	cross section area of damaged structure
b	cell width
$\mathbf{D}$	impedance matrix
E	Young's modulus
F_t	external force
H	FRF vector
H_d	damaged FRF vector
h	distance between the measurement points
h_c	cell thickness
I	area moment of inertia
k_F	bending wavenumber
k_L	wavenumber
L	length of the cell
M_t	internal transverse shear force
p	damage magnitude
Q_t	internal out-of-plane force
$\mathbf{R}$	receptance matrix
$\mathbf{T}$	transfer matrix
$\mathbf{T}_{cell}$	cell transfer matrix

$\mathbf{T}_D$	transfer matrix of damaged periodic model
$\mathbf{T}_{total}$	transfer matrix of the periodic model
t	time
U	displacement
u	longitudinal displacement
w	transverse displacement
x	spatial coordinate

Greek symbols

δ	attenuation constant
ϵ	phase constant
ρ	mass density
ω	frequency
ω_n	natural frequency

Abbreviations

DOF	Degrees of freedom
FRAC	Frequency Response Assurance Criterion
FRF	Frequency Response Function
SDIM	Structural Damage Identification Method
SEM	Spectral Element Method
SHM	Structural Health Monitoring

Chapter 1

Introduction

In this first chapter, a literature review of the main topics of this study is introduced. The objectives and the dissertation structure are also defined.

1.1 Background on the identification of damage

In the field of structural dynamics, an important subject is structural damage detection. Inman et al. (2005) covered the study on structural health monitoring that helped the damage prognosis problems. During the development phases of structural projects, dynamic behavior must be known, because failures occur due to not knowing the characteristics of the structure as its dynamic response. These can be caused by the application of repetitive loads as well, which are directly involved with fatigue, crack propagation, and accumulation of structural damage. Mechanical components tend to react to stimuli, such as stress caused by static and dynamic loads.

In general, most types of structures are subjected to different internal and external factors that cause damage and malfunction which can be due to corrosion wear, deterioration due to lack of quality control, or an extreme situation such as just because of the environmental influence. Because of that, a damage identification system is essential, detecting anomalies in maintenance time, reducing accident risks, and reducing costs.

According to Farrar et al. (2006), intelligent structures are systems that integrate sensors, actuators and controllers. These structures can be part of aircraft, automobiles and ships with networks of sensors and actuators that would allow these structures to react to changes in the environment actively. Such structures are inspired by nature, where they seek to reproduce the adaptive characteristics of natural systems; that is, these structures must respond to external and internal excitations properly.

The industry has been demanding more and more improvements in the detection of vibrations in structures to reduce fatigue failure and improve the dynamic behavior of the structure to achieve greater system stability. The study of intelligent structures has been encouraging structural optimization techniques, sensors, and controllers. The combined use of these generates a system for better control of external excitations. According to Farrar and Worden (2007), the failure prognosis process evaluates the current state of the structure, estimates the operating conditions to which this structure will be subjected and, based on simulations, the remaining useful life is predicted.

The Structural Health Monitoring (SHM) is a prognostic failure phase, evaluating the present state of the structure. The SHM seeks to perform measurements of the dynamic response of a system continuously, from sensors installed in the structure. The extracted data become sensitive to the presence of the damage, altering the measured values; these are analyzed statistically for the determination of the current state of the system in relation to its integrity. For Doebling et al. (1998), the purpose of a monitoring system should be to accumulate enough information about the damage that occurred to take appropriate actions to restore the correct performance of the structure or at least ensure security.

1.2 Damage detection methods

Changes in structural dynamic characteristics such as mode shapes, natural frequencies, vibration responses, and modal damping values, show the presence of damage in the structure. Thus, these quantities are used to support the detection, localization, and quantification of these damages.

In the literature, several studies investigated different methods that are more effective for the identification of structural damage. Lee and Shin (2002) presented a frequency response function (FRF) based structural damage identification method (SDIM) for beam structures, where the feasibility of the method was verified. They used strategies to define the problem of detecting positioned damage, such as: obtaining FRF equations, varying excitation frequency, and the measurement point of the dynamic response; and reduce the problem domain.

Another strategy is the transmissibility method, studied by Chesné and Deraemaeker (2013). In this paper, the transmissibility functions were used to detect damage. They use frequency bands to locate damage, as they are sensitive to changes in the structure. The main problem encountered by them is that to understand the behavior of a damaged structure, it is necessary to have several frequency ranges for different types of damage, which is rarely available.

The spectral finite element method was analyzed in study by Ostachowicz (2008), who showed that this method is more sensitive in detecting the damage. The location of the damage is only allowed when there is a difference between the measured signals of the damaged structure and the undamaged structure. This study demonstrated to be more realistic in engineering applications because it was possible to detect very small cracks.

Other methods contribute to the identification of damages, Marwala and Heyns (1998) studied the use of the multiple criterion method, that it was compared with the frequency response function method and with the modal property based method, showed by Allemang and Brown (1982). The method predicts the presence, position, and intensity of the damage.

Kimsan et al. (1998) used the FRF curvature difference method to locate structural damage. This method has advantages as the numerical error in the curve adjustment can be eliminated and it is not necessary to obtain the modal parameter. To ensure the efficiency of this method, the sensitivity must be adjusted, as this is crucial for the location and the level of damage. This study also showed that the FRF difference in curvature is sensitive to damage, which is higher for a high level of damage. The research of Reddy and Swarnamani (2012) showed the effectiveness of using the FRF to identify damage. Applying the FRF curvature method, it was concluded that the influence of the excitation location is not important for damage detection.

The article of Mohammadirad et al. (2018) proposes a study of the effectiveness of using the Frequency Response Guarantee Criterion (FRAC) to identify failures in a system. The results are shown in the same noisy environment or the effective method for detecting the presence of damage.

1.3 Periodic structures

Knowing that the growth of damage to structural elements is a significant problem, the present work studies its behavior in periodic structures. Periodic structures are systems that have repeated sub elements, combined in a tandem manner. For Mead (1996), a periodic structure is a structure composed of structural components arranged in regular arrays such as mass and springs. The Figure 1.1 shows an arrangement of elements presented as an example of a periodic system in the study of Mead (1975).

Figure 1.1: Diagram of a one-dimensional periodic system Mead (1975).

Besides, periodic structures can have one, two, or three dimensions, consisting of bars, beams, plates, shells, or different combinations of these. In engineering, examples of periodic structures are solar panels, satellite panels, airplane wings and fuselages, oil pipelines, train tracks, and many others. As the Figure 1.2a shows, the first image is the fuselage of an airplane, where its structural components are repeated numerous times. In Figure 1.2b, a satellite panel has periodicity along its length. And in Figure 1.2c, it shows that the parts of the train track are similar.

The elements in periodicity present band gaps, which are frequency bands in which there is no propagation of the waves in the structure, thus aiding in the control of noise and vibrations. An interesting characteristic of its dynamic behavior is the formation of stopband and passband regions, that is attenuation and propagation region. In the Figure 1.3, the attenuation and propagation regions are shown.

Considering a periodic structure, the upper part of the Figure 1.3 presents the frequency response of this type of structure. The graph in the middle of the Figure 1.3 indicates the

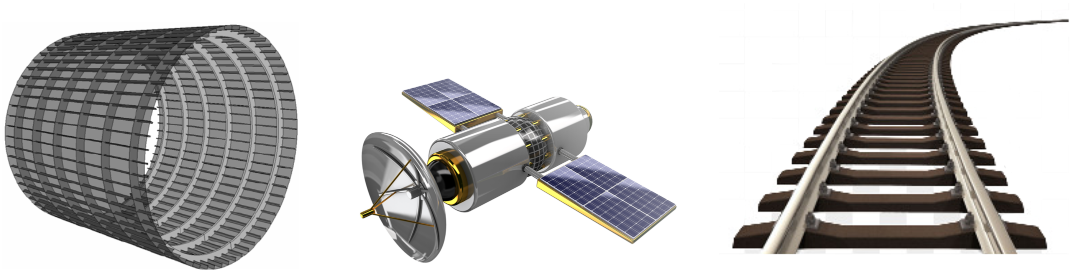

(a) (b) (c)

Figure 1.2: Examples of periodic structure: (a) airplane fuselages from Scientific Diagram (Acess 2020-04-22a) (b) satellite panels from Scientific Diagram (Acess 2020-04-22b) and (c) train tracks from DLPNG (Acess 2020-04-22).

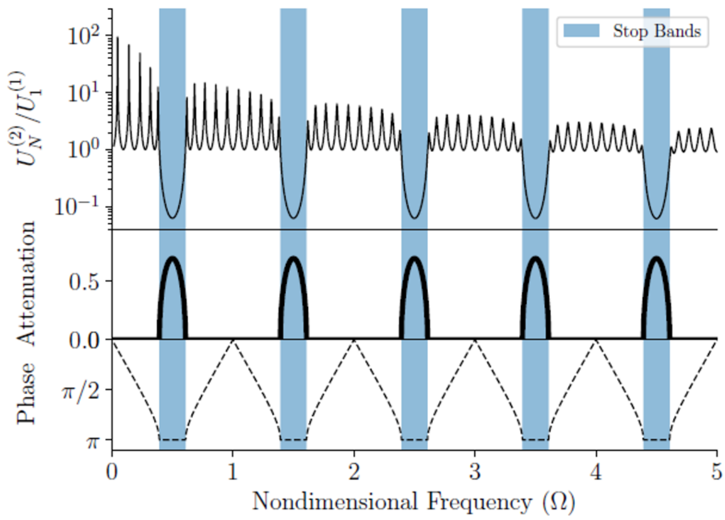

Figure 1.3: Diagram of frequency, attenuation and phase of periodic bar.

regions of attenuation. And the bottom part of the Figure 1.3 shows the phases of this arrangement. The regions marked in blue indicate the stopbands regions, where there is no wave propagation, or where the propagation is attenuated.

As stopband regions, characteristics of periodic structures can be further investigated to use these applications in engineering. (Olhoff et al., 2012) used the concept of maximizing frequency gaps to study the behavior of beam structures. Some studies, (Xiang and Shi, 2009), determined the stopband in flexural beam vibration in periodicity. In this area, the wave movement and its propagation are attractive means for analysis. Wave dispersion studies have been a topic of great interest over the past 20 years. The dispersion analysis of the periodic structures are concentrated mainly in this area. Tassilly (1987) and Liang et al.

(2017) studied the dispersion relationship between the number of waves and the frequency of a class of non-uniform periodic elements. In the field of vibrations, energy band analysis and dynamic responses of structures with periodicity have been highlighted in many studies.

Because of the greater the number of elements in a structure, the greater the computational time of analysis. As the periodic structure has identical elements, the solution is faster, but the efficiency is not ideal. Therefore, other considerations, (Kangwai et al., 1999), have investigated effective tools for greater computational efficiency. One of the means found to simplify the problem is to make the elements symmetrical, (Wanxie and Chunhang, 1983). The methods using the complete stiffness matrix have been converted to a rearrangement form to facilitate the representation of the group of elements, and this technique was applied to symmetrical structures, (Kangwai and Guest, 2000). An efficient algorithm to solve dynamic responses of one-dimensional and two-dimensional periodic structures was an (Liang et al., 2017) study.

In the study of Rubin (1967) , the concept of immittance and transmission matrices applied in mechanical systems was presented, showing the relationships between these formulas. The admittance matrices present as a response velocities, where its input is forces. And the impedance matrix is the inverse of admittance. The transmission matrix is one which velocities and forces as input and output. It may be applied for a series of connected elements, where the output of the first element is equal to the input in the second, and so on. The main characteristic of this matrix is the possibility of multiplying the transmissibility matrices of each part, consequently obtaining the transmissibility matrix of the complete set.

The Impedance method was studied by Ungar (1966), who represented the vibration of a uniform beam allowing the analysis of the structures with loads. Later, Gupta (1970) presented an analysis for the periodic beams introducing the concept of cell and transfer matrix. The propagation and attenuation parameters are now used in the study of periodicity in structures. The incident wave in a medium with different characteristics, such as geometry, is known to be segmented into the propagated wave and reflected wave. If the periodicity varies, the boundaries of the passband and stopband regions are mixed. So if there is an irregularity in the structure, a part of the wave does not propagate, characterizing the destructive interference of the passband.

Mead (1975) presented the damping effect on the periodic structure. While Langley (1994) used the damped periodic structures to locate the wave. The localization of a source has always been in focus in the context of mechanical wave propagation; the transfer method was introduced by Kissel (1991) to identify them using random disorder.

1.4 Research objetives

The purpose of this work is analyze the influence of structural damage in one-dimensional periodic structures such as bars and beams. Initially, the study is based on a structure with symmetric periodic cells and understand its behavior. After that, it is proposed to simulate damage in different positions of the cells in the periodic structure and to analyze the influence of the damage in the structure. To simulate the damage, the cross section of some elements are varied, representing a wear effect, or loss of stiffness. Therefore, the main objectives to be achieved in this work are:

- to model one dimensional periodic structures using the exact solution of wave equations;
- to understand the behavior of periodicity in bar and beams analyzing the characteristics of the response;
- to simulate the damage in different cell positions and understand the behavior of the damage in the dynamic response of the system;
- to use comparison methods to improve damage identification.

1.5 Dissertation outline

In this first chapter, the bibliographical review of the main topics studied in this work was detailed. In chapter 2, the mathematical models introduced in the previous sections will be implemented using the transfer matrix and dynamic stiffness method. Later, in chapter 3, a periodic model was developed with symmetric cells. Later, an undamaged periodic system was modelled. Then the damage was introduced to the model to represent a damaged structure.

The numerical analyzes are in chapter 4, showing the results achieved in the work. Those show the behavior of the system and the methods implemented to identify the damage in the system. In the last chapter, conclusions about the results obtained in the previous chapter are shown, and a plan of activities is written for the next steps leading to the conclusion of this project.

Chapter 2

System modeling

This chapter presented the procedure used to model unidimensional systems such as beam and bars using spectral element method, as proposed by Lee (2009). These models correspond to a single element represented by the dynamics stiffness or receptance matrices. These representations are later converted to a transfer matrix format, such that an array of periodic element can be obtained by the multiplication of single elements.

The Spectral Element Method (SEM) is similar to the Finite Element Method (FEM), however, SEM is written in the frequency domain and the element interpolation is the analytical solution of the wave equation. As shown by Doyle (2012), the Spectral Element Method was formulated for elements such as bar, beam and plate.

2.1 Longitudinal vibration of bars

In this section, the method of spectral element formulation for bars are introduced. Considering a free longitudinal vibration of a uniform bar, Figure 2.1.

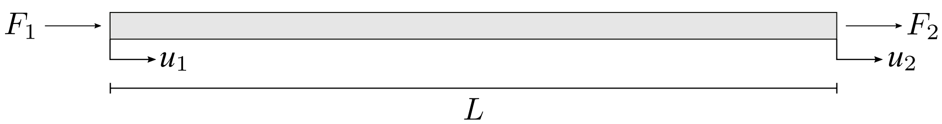

Figure 2.1: Bar element with length L with the forces and displacements acting at both ends.

The equation that governs the dynamic displacement of a free longitudinal vibration of a uniform bar is represented as

$$EAu^{''} - \rho A\ddot{u} = 0 \tag{2.1}$$

in which $u(x,t)$ is the longitudinal displacement, E is the Young's Modulus, A is the cross-section area, ρ is the mass density, and $F_t(x,t)$ is an external force. The dots (.) denote the derivatives with respective to time t. And the superscript ($'$) denotes the derivatives with respective to spatial coordinate x. Thus, assuming the spectral solution of the form

$$u(x,t) = \frac{1}{N}\sum_{n=0}^{N-1} U_n(x;\omega_n)e^{i\omega_n t} \tag{2.2}$$

in which $U_n(x;\omega_n)$ is the Fourier coefficient limited to $n = 0$ up to the number of samples N, ω_n is the natural frequency and t is time. Substituting Eq. 2.2 into Eq. 2.1, allows writing

$$EAU^{''} + \omega^2 \rho AU = 0 \tag{2.3}$$

The solution for Eq. 2.3 can be given by

$$U(x) = ae^{-ik(\omega)x} \tag{2.4}$$

Thus, replacing Eq. 2.4 in Eq. 2.3, the dispersion relation is found and the wavenumber k_L is obtained as

$$k_L = \omega\sqrt{\frac{\rho}{E}} \tag{2.5}$$

Assuming a finite bar element of length L, Figure 2.1, the general solution of the model is obtained and the boundary conditions, nodal DOF, are implemented to define the spectral element matrix.

$$\mathbf{D}_{bar}(\omega) = \frac{EA}{L}\begin{bmatrix} D_{11} & D_{12} \\ D_{21} & D_{22} \end{bmatrix} \tag{2.6}$$

in which

$$D_{11} = D_{22} = k_L L \cot(k_L L)$$
$$D_{12} = D_{21} = -k_L L \csc(k_L L)$$

2.2 Bending vibration of beams

In this second section, the method of spectral element formulation for beams are introduced. To add to the study, the beam element will also be developed. The free bending vibration of a beam is represented by

$$EIW^{''''} + \rho A\ddot{w} = 0 \tag{2.7}$$

in which $w(x,t)$ is the transverse displacement, E is the Young's modulus, I is the area moment of inertia, A is the cross-section area, ρ is the mass density and $F(x,t)$ is an external force. The internal transverse shear force and bending moment are represented by

$$M_t(x,t) = EIw^{''}(x,t) \tag{2.8}$$
$$Q_t(x,t) = -EIw^{'''}(x,t) \tag{2.9}$$

Similarly to what was done for the bar. The solution of Eq. 2.8 in spectral form is given by

$$w(x,t) = \frac{1}{N}\sum_{n=0}^{N-1} W_n(x;\omega_n)e^{i\omega_n t} \tag{2.10}$$

Replacing Eq. 2.10 in Eq. 2.8, allows writing

$$EIW^{''''} - \omega^2 \rho A W = 0 \tag{2.11}$$

So, the general solution of Eq. 2.11 is given by

$$W(x) = ae^{-ik(\omega)x} \tag{2.12}$$

Substituting Eq. 2.12 in Eq. 2.11, the wavenumber, k_F is obtained

$$k_F = \sqrt{\omega}\left(\frac{\rho A}{EI}\right)^{\frac{1}{4}} \tag{2.13}$$

The two solutions found for the number of waves are also called beam propagating and non-propagating modes. Assuming a finite beam element of length L, Figure 2.2, the general solution of the model is obtained and the boundary conditions, nodal DOF, are implemented to define the spectral element matrix.

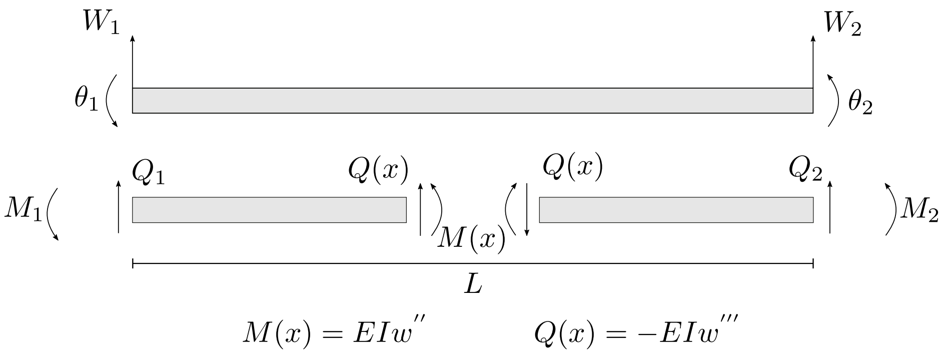

Figure 2.2: Beam element with length L and the respective forces, moments, displacement and angular displacement.

$$\mathbf{D}(\omega) = \frac{EI}{L^3}\begin{bmatrix} d_{11} & d_{12} & d_{13} & d_{14} \\ d_{21} & d_{22} & d_{23} & d_{24} \\ d_{31} & d_{32} & d_{33} & d_{34} \\ d_{41} & d_{42} & d_{43} & d_{44} \end{bmatrix} \tag{2.14}$$

in which

$$
\begin{aligned}
&d_{11} = d_{33} = \Delta b k_F L^3(\cos(k_F L)\sinh(k_F L) + \sin(k_F L)\cosh(k_F L))\\
&d_{22} = d_{44} = \Delta b k_F L^3(-\cos(k_F L)\sinh(k_F L) + \sin(k_F L)\cosh(k_F L)\\
&d_{12} = -d_{34} = \Delta b k_F L^3 k_F^{-1}\sin(k_F L)\sinh(k_F L)\\
&d_{13} = \Delta b k_F L^3(\sin(k_F L) + \sinh(k_F L))\\
&d_{14} = -d_{23} = \Delta b k_F L^3 k_F^{-1}(-\cos(k_F L) + \cosh(k_F L))\\
&d_{24} = \Delta b k_F L^3 k_F^{-1}(-\sin(k_F L) + \sinh(k_F L))\\
&\Delta b = \frac{1}{1-\cos(k_F L)\cosh(k_F L)}
\end{aligned}
$$

The spectral element matrix for a bar and a beam is defined in Eq. 2.6 and Eq. 2.14, respectively. These matrices are impedance matrices, which shows the relation between forces and displacement.

2.3 Impedance matrix

The following mathematical analysis is made for a bar, since from its more complex structures, like beams, are based on the equations. The impedance matrix for a bar element, $\mathbf{D}_{bar}$, is given by

$$\mathbf{F}(\omega) = \mathbf{D}_{bar}\mathbf{U}(\omega) \tag{2.15}$$

The inverse of impedance is receptance, $\mathbf{R}$. For the numerical analysis, Receptance matrix is obtained, as the force vectors , $\mathbf{F}$ are input and the displacements, $\mathbf{U}$ are the output.

$$\mathbf{U}(\omega) = \mathbf{R}\mathbf{F}(\omega) \tag{2.16}$$

These matrices are symmetrical, due to the principle of reciprocity. Another way to represent association of displacement and forces is the Transfer Matrix. The Transfer Matrix, $\mathbf{T}$ is the relationship between two ends of a structural element connected by nodes, interaction of forces and displacements.

$$\begin{Bmatrix} F_2 \\ U_2 \end{Bmatrix} = \mathbf{T} \begin{Bmatrix} F_1 \\ U_1 \end{Bmatrix}, \text{ or given in compact form: } \psi_2 = \mathbf{T}\psi_1 \tag{2.17}$$

For a bar element, the impedance representation can be transformed into a transfer matrix for by the method shown by Rubin (1967), relating the force state vectors and displacements at each end by

$$\begin{Bmatrix} U_2 \\ F_2 \end{Bmatrix} = \begin{bmatrix} -D_{11}D_{21}^{-1} & -D_{11}D_{21}^{-1}D_{22} + D_{12} \\ -D_{21}^{-1} & D_{21}^{-1}D_{22} \end{bmatrix} \begin{Bmatrix} U_1 \\ F_1 \end{Bmatrix} \tag{2.18}$$

And the reverse process, transforming the transfer matrix into an impedance matrix is also valid. Considering the transfer matrix in a simplified way, the arrangement of the internal components is given by

$$\begin{Bmatrix} U_2 \\ F_2 \end{Bmatrix} = \begin{bmatrix} A & B \\ C & D \end{bmatrix} \begin{Bmatrix} U_1 \\ F_1 \end{Bmatrix} \longrightarrow \begin{Bmatrix} F_1 \\ F_2 \end{Bmatrix} = \begin{bmatrix} -C^{-1}D & C^{-1} \\ (C^{-1})^T & -AC^{-1} \end{bmatrix} \begin{Bmatrix} U_1 \\ U_2 \end{Bmatrix} \tag{2.19}$$

The transfer matrix is used to facilitate the multiplication of identical elements of the periodic structure. However, the transformation of the transfer matrix into an impediment matrix is necessary to obtain the final dynamic response of the system. This rearrangement of matrix components aims to make possible the simpler analysis of a complex structure.

$$\begin{Bmatrix} U_2 \\ F_2 \end{Bmatrix} = \mathbf{T} \begin{Bmatrix} U_1 \\ F_1 \end{Bmatrix} \longrightarrow \begin{Bmatrix} F_1 \\ F_2 \end{Bmatrix} = \mathbf{D}_{bar} \begin{Bmatrix} U_1 \\ U_2 \end{Bmatrix} \tag{2.20}$$

The impedance, receptance and transfer matrices contain similar information, but with different arrangements.

2.4 Behavior of periodic structures

The main focus of this strategy is the dynamic behavior of periodic structures. Several methods assist in the mathematical modeling of dynamic systems, but for this study two methods were chosen. The first method used is the Transfer Matrix, which only needs the input of the first cell to get the answer at the output of the last cell. The second method used is the rearrangement of the Dynamic Stiffness Matrix, which responds to the output of any cell belonging to the structure.

The transfer matrix is a 2x2 matrix, where the inputs and outputs refer to the first and last cell of a periodic structure.

$$\begin{Bmatrix} F_{n_{cell}} \\ U_{n_{cell}} \end{Bmatrix} = \mathbf{T} \begin{Bmatrix} F_1 \\ U_1 \end{Bmatrix} \tag{2.21}$$

So, when this analysis is used, it is necessary to know only the cell transfer matrix that will be repeated, in order to obtain the final response of the periodic model. However, if it is necessary to analyze a cell inside the model, the transfer method is not useful. The dynamic stiffness matrix has the number rows and columns according to the number nternal degrees of freedom. This means that the bigger the number of cells, the greater the size of the dynamic stiffness matrix. In this way, it is possible to analyze the response of each cell, using the rows and columns of the total dynamic stiffness matrix of the periodic structure, as will be shown in this chapter.

According to Mead (1999), the eigenvalues of the transfer matrix for a unit cell are related to the propagation constants and phase, which indicate the frequency regions where stop and pass band occurs. To understand its behavior, a periodic bar/beam consisting of 15 cells was analyzed, Figure 2.3. This model presents the properties of Aluminum, and the cell length is 0.1 m. The total length is 1.5m.

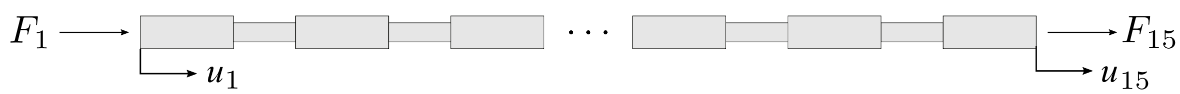

Figure 2.3: Model of periodic structure with 15 cells.

In the attenuation and propagation zones, the motion in a cell is equal to $e^{-\delta \pm i\varepsilon}$ times the displacement in the next cell. The complex propagation constant of the wave motion at the periodicity is $e^{-\delta \pm i\varepsilon} = \mu$. δ is the attenuation constant and ε is the phase constant. For Mead (1999), there are two parts that vary with frequency, Figure 2.4 and 2.5, where only the negative values of ε are presented. In the propagation zones, the attenuation constant is zero and the phase constant varies with frequency. In the attenuation zones, the phase constant is zero or π while attenuation constant varies.

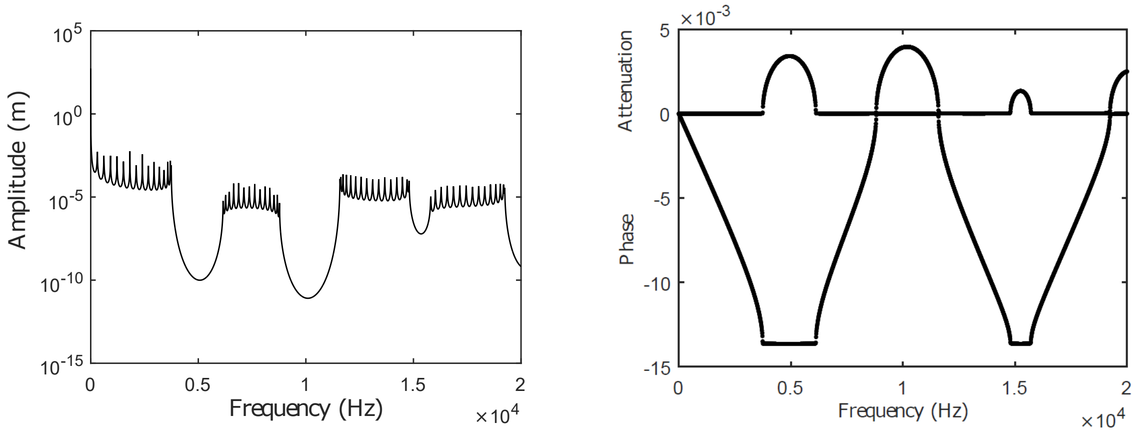

(a) (b)

Figure 2.4: (a) Frequency response of the periodic bar (Longitudinal vibration). 1N force applied to the first cell of the periodic structure and measured to the last cell (cell 15). (b) Phase and attenuation of the periodic bar.

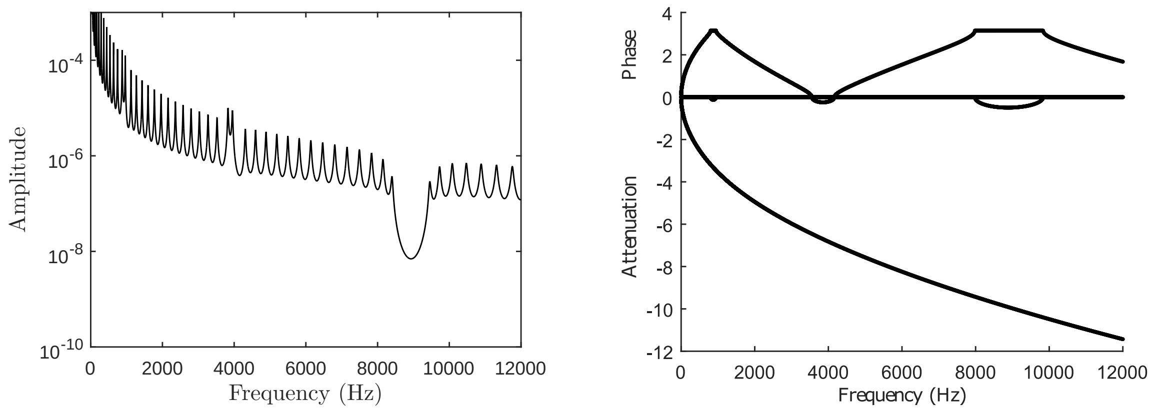

Figure 2.5: (a) Frequency response of the periodic beam (Bending vibration). 1N force applied to the first cell of the periodic structure and measured to the last cell (cell 15). (b) Phase and attenuation of the periodic beam.

2.4.1 Using the transfer matrix method

The use of transfer matrix method, allows the calculation of the structural response of tandem system. Such that the composition of a series of elements is obtained by the multiplication of the transfer matrices of the individual elements. So, to explain it better, consider a cell with three bars with different lengths, L_1, L_2 and L_3.

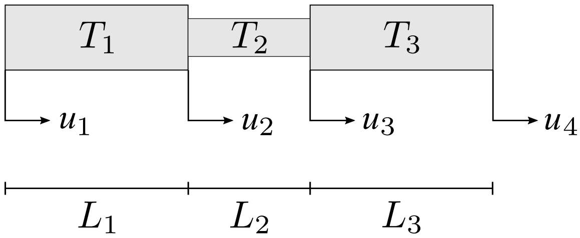

Figure 2.6: Representation of a single cell consisting three rod segments with different cross section areas.

This method consists of a transfer matrix for each substructure. Thus, the dynamic response of the complete structure is the multiplication of the substructure transfer matrices.

So, with the transfer matrix of each element it is possible to obtain the matrix of the unit cell, the transfer matrix of one cell can be obtained by

$$\mathbf{T}_{cell} = \mathbf{T}_3\mathbf{T}_2\mathbf{T}_1 \tag{2.22}$$

$$\begin{bmatrix} F_4 \\ U_4 \end{bmatrix} = \mathbf{T}_3\mathbf{T}_2\mathbf{T}_1 \begin{bmatrix} F_1 \\ U_1 \end{bmatrix} \tag{2.23}$$

in which $\mathbf{T}_1$ is the transfer matrix for the section of the cell with length L_1, $\mathbf{T}_2$ is the transfer matrix of the section of the cell with length L_2, and $\mathbf{T}_3$ is the transfer matrix of the section of the cell with length L_3.

The model used in this analysis is symmetrical, the first and the third element equal. So the transfer matrix of the cell becomes

$$\mathbf{T}_{cell} = \mathbf{T}_1\mathbf{T}_2\mathbf{T}_1 \tag{2.24}$$

This method helps to model a periodic structure, the matrix system is further simplified because the structures are identical, and the matrix is repeated.

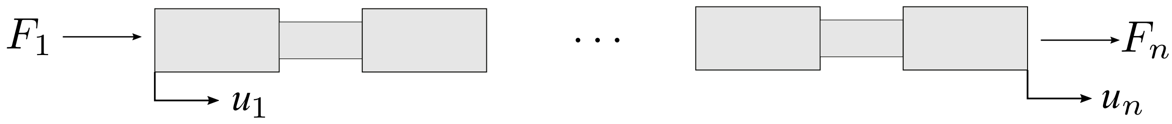

Figure 2.7: Model of periodic bar with n elements

$$\mathbf{T}_{total} = \mathbf{T}_1\mathbf{T}_2\cdots\mathbf{T}_n \tag{2.25}$$

in which n is the number of elements in the structure. The matrix $\mathbf{T}_{total}$ represents the whole structure relating the left and right hand side of the beam.

As the cell is repeated numerous times, the transfer matrix of the periodic model proposed in this work is compacted

$$\mathbf{T}_{cell} = (\mathbf{T}_1\mathbf{T}_2\mathbf{T}_1)^{n_{cell}} \tag{2.26}$$

in which n_{cell} is the number of periodic cells in the structure.

2.4.2 Using the dynamic stiffness

The higher the number of cells, the dynamic stiffness matrix becomes bigger. And therefore, the longer the analysis time and obtaining information will be time consuming. The objective of the following method is to reduce the size of the overall dynamic stiffness matrix, taking into account that the forces are applied only to the ends of the structure.

When a system with more elements is analyzed, a dynamic stiffness matrix becomes much more complex. Consider a periodic model represented with the interaction of the right (R), internal (I), and left (L) nodes.

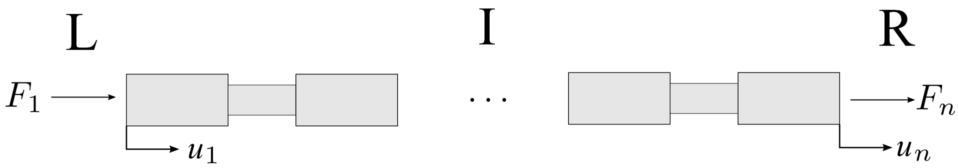

Figure 2.8: Representation of a periodic bar with n elements with left, internal, and right nodes interaction.

Considering a structure with n elements, Figure 2.8, a dynamic stiffness matrix is given by

$$\begin{bmatrix} F_1 \\ F_2 \\ \vdots \\ F_{n-1} \\ F_n \end{bmatrix} = \begin{bmatrix} D_{1,1} & D_{1,2} & \cdots & D_{1,n-1} & D_{1,n} \\ D_{2,1} & D_{2,2} & \cdots & D_{2,n-1} & D_{2,n} \\ \vdots & & \ddots & & \vdots \\ D_{n-1,1} & D_{n-1,2} & \cdots & D_{n-1,n-1} & D_{n-1,n} \\ D_{n,1} & D_{n,2} & \cdots & D_{n,n-1} & D_{n,n} \end{bmatrix} \begin{bmatrix} U_1 \\ U_2 \\ \vdots \\ U_{n-1} \\ U_n \end{bmatrix} \tag{2.27}$$

The first step in the matrix rearrangement is to change the line referring to F_1, which is to change the first line in the penultimate line of the matrix.

$$\begin{bmatrix} F_2 \\ \vdots \\ F_{n-1} \\ F_1 \\ F_n \end{bmatrix} = \begin{bmatrix} D_{2,1} & D_{2,2} & \cdots & D_{2,n-1} & D_{2,n} \\ \vdots & & \ddots & & \vdots \\ D_{n-1,1} & D_{n-1,2} & \cdots & D_{n-1,n-1} & D_{n-1,n} \\ D_{1,1} & D_{1,2} & \cdots & D_{1,n-1} & D_{1,n} \\ D_{n,1} & D_{n,2} & \cdots & D_{n,n-1} & D_{n,n} \end{bmatrix} \begin{bmatrix} U_1 \\ U_2 \\ \vdots \\ U_{n-1} \\ U_n \end{bmatrix} \tag{2.28}$$

The second step is to change the column for U_1, which is to change the first column in the penultimate column.

$$\begin{bmatrix} F_2 \\ \vdots \\ F_{n-1} \\ F_1 \\ F_n \end{bmatrix} = \begin{bmatrix} D_{2,2} & \cdots & D_{2,n-1} & D_{2,1} & D_{2,n} \\ \vdots & \ddots & \vdots & \vdots & \vdots \\ D_{n-1,2} & \cdots & D_{n-1,n-1} & D_{n-1,1} & D_{n-1,n} \\ D_{1,2} & \cdots & D_{1,n-1} & D_{1,1} & D_{1,n} \\ D_{n,2} & \cdots & D_{n,n-1} & D_{n,1} & D_{n,n} \end{bmatrix} \begin{bmatrix} U_2 \\ \vdots \\ U_{n-1} \\ U_1 \\ U_n \end{bmatrix} \tag{2.29}$$

Therefore, the main matrix is subdivided into six shorter matrices of different sizes. Each smaller matrix represents the interaction of the right (R), internal (I), and left (L) nodes.

$$\begin{bmatrix} F_2 \\ \vdots \\ F_{n-1} \\ F_1 \\ F_n \end{bmatrix} = \begin{bmatrix} [\widehat{D}_{II}]_{n-2\times n-2} & [\widehat{D}_{IL}]_{n-2\times 1} & [\widehat{D}_{IR}]_{n-2\times 1} \\ [\widehat{D}_{LI}]_{1\times n-2} & \widehat{D}_{LL} & \widehat{D}_{LR} \\ [\widehat{D}_{RI}]_{1\times n-2} & \widehat{D}_{RL} & \widehat{D}_{RR} \end{bmatrix} \begin{bmatrix} U_2 \\ \vdots \\ U_{n-1} \\ U_1 \\ U_n \end{bmatrix} \tag{2.30}$$

The main matrix used in this study is given by

$$\mathbf{D} = \begin{bmatrix} \widehat{D}_{LL} & \widehat{D}_{LR} \\ \widehat{D}_{RL} & \widehat{D}_{RR} \end{bmatrix} \tag{2.31}$$

in which

$$\widehat{D}_{LL} = \widehat{D}_{LL} - \widehat{D}_{LI}\widehat{D}_{II}^{-1}\widehat{D}_{IL} \tag{2.32}$$

$$\widehat{D}_{LR} = \widehat{D}_{LR} - \widehat{D}_{LI}\widehat{D}_{II}^{-1}\widehat{D}_{IR} \tag{2.33}$$

$$\widehat{D}_{RL} = \widehat{D}_{RL} - \widehat{D}_{RI}\widehat{D}_{II}^{-1}\widehat{D}_{IL} \tag{2.34}$$

$$\widehat{D}_{RR} = \widehat{D}_{RR} - \widehat{D}_{RI}\widehat{D}_{II}^{-1}\widehat{D}_{IR} \tag{2.35}$$

Acknowledging that each matrix is the relationship between the nodes, where the internal nodes are not known. The matrix formed by the last values is the relationship between the nodes on the right and the nodes on the left. Since these nodes are recognized, input and output nodes, this matrix is used in the process. This dynamic stiffness matrix is used to transform in transfer matrix by the method show in Eq.2.18.

2.5 Chapter remarks

In this second chapter, a mathematical model of a periodic structure was developed, using the Spectral Element Method (SEM). Its behavior was analyzed, identifying the regions of attenuation and wave propagation. The periodicity was introduced in the model using the transfer and dynamic stiffness matrices, showing a method of rearranging the dynamic stiffness matrix for a system with many elements.

Chapter 3

Damage identification metrics

The characteristics of the structure affect its dynamic response. One way to identify, locate and quantify structural damage is to understand its behavior and characteristics, such as natural frequency, mode shape, and modal damping. There are many studies of methods for effective damage detection, which are called Structural Damage Identification Methods (SDIMs).

This chapter uses the modal data, impedance matrix, frequency response function (FRF) data, and transfer matrix to support structural damage identification. Using the spectral element method (SEM) in association with transfer and dynamic stiffness matrix, the FRF data was analyzed to identify the damage.

It is important to highlight the difficulty in detecting damage in a structure, as it depends not only on its size but also on its position. If the damage is very small to the size of the entire structure, or if the damage is closer, in the middle or distant from the excitation of the system, the dynamic response may be sensitive or insensitive to this variation.

As is known, the damage is not uniform, nor is its location, shape or size known, that is, it is not possible to represent the precise stiffness of the damaged structure. Then, to represent the damaged structure in this study, an approach of its cross section area is applied.

$$A_D = A(1 - p) \tag{3.1}$$

in which A is cross section area for an intact structure and A_D is cross section area for a damaged structure. In this case, p is the damage magnitude, where $p = 0$ represent the structure without damage, and when $p = 1$ there is a rupture of the material.

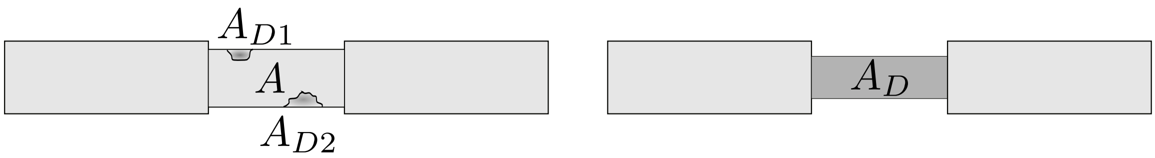

Figure 3.1: Structure with localized damage and structure with the representation of uniform damage

The first structure of the Figure 3.1 represents the structure with local damage. The structure has its cross section area, A, and each damage (corrosion) has its respective cross section area, A_{D1}, and A_{D2}. Though, the second part of the Figure 3.1 presents the structure with uniform damage, A_D, that is, a rearrangement of cross section area of the undamaged structure to those of the damages. And this cross section area, A_D, becomes smaller.

For this study, the damage was simulated as a decrease in the area in the central element of the periodic cell. As proposed in Chapter 2, the periodic cell is symmetrical.

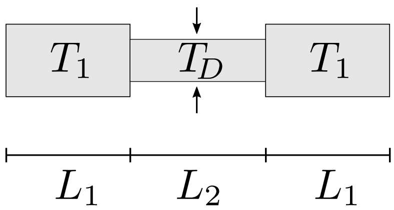

Figure 3.2: Model of periodic cell with a damage

The transfer matrix of damaged element is represented by $\mathbf{T}_D$. So, the transfer matrix that represents this cell is given by

$$\mathbf{T}_{damage} = \mathbf{T}_1 \mathbf{T}_D \mathbf{T}_1 \tag{3.2}$$

The damage is included in only one element of the periodic structure. And so, by simulating damage at a location in the structure, the dynamic response is analyzed.

In this way, the transfer matrix for the entire structure is given by

$$\mathbf{T}_{total} = \mathbf{T}_{cell} \mathbf{T}_{damage} (\mathbf{T}_{cell})^N \tag{3.3}$$

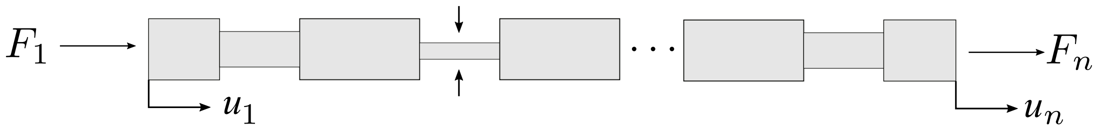

Figure 3.3: Model of periodic structure with damage

The position of the damage transfer matrix changes according to the position of the damage in the cell. In this case, the damage is in the second cell, so its matrix must to be in the second position of Eq. 3.3. The formulation of $\mathbf{T}_{cell}$ is in Chapter 2.

3.1 Correlation methods

In this section, the correlation methods are presented. These have been studied for over 20 years, these are used to qualitatively compare a reference model with a modified model. In this strategy, correlation methods were used to compare the structure without damage to the damaged structure, looking for the location of the damage. These types of methods are often used to validate dynamic models.

These are used to assist in the identification of damages in the final phase of the analysis. After finding the dynamic stiffness matrix of the structure with the damage inserted, the correlation methods help to locate and quantify the damage in the structure. So, based on the analytical data in this study, it was possible to compare the models without damage and with damage.

Two methods were used in the analysis of this work, the Frequency Response Assurance Criterion (FRAC) and the Frequency Response-Function Curvature Method. And for both methods, the periodic bar/beam has the pre-defined properties as shown in Tab. 3.1.

Table 3.1: Bar/Beam Properties used in the Numerical Simulations

Property	Value
Cell length L_{cell}	0.1 m
Thickness h_c	4.3 $\times 10^{-3}$ m
Width b	13 $\times 10^{-3}$ m
Young's Modulus E	70 GPa
Density	2710 kg

The three-element cell is made of only one material, Aluminum.

3.1.1 Frequency response assurance criterion

Heylen and Lammens (1996), Fregolent and D.Ambroglo (1997) and Nefske and Sung (1996) showed in the frequency response functions representing the same input-output relationship can be compared using a technique known as the frequency response assurance criterion (FRAC). So, as the two models compared (damaged and undamaged) present the same boundary conditions, the FRAC becomes valid. This method can be compared as FRFs in entire or partial data, as long as the models are in the same frequency range. The FRAC can be calculated as Eq.3.4:

$$FRAC = \frac{|H{H_d}^T|^2}{|H|^2|H_d|^2} \tag{3.4}$$

in which H is the undamaged FRF vector and H_d is the damaged FRF vector.

The FRAC depends on the frequency function, correlates the frequency response, which depends on the iteration of all individual modes. The FRAC assumes values between 0 and 1. When the FRAC has a value of 1, it means that the correlation is perfect, all the FRF values compared are the same. Thus, the structure is undamaged. Any value between 0 and 1 shows the presence of a change in the structure. To compare FRF values, use the entire set or a partial set of FRF data.

In the FRAC analysis, the dynamic stiffness matrix is obtained by the transfer method, since only the input and output values are needed.

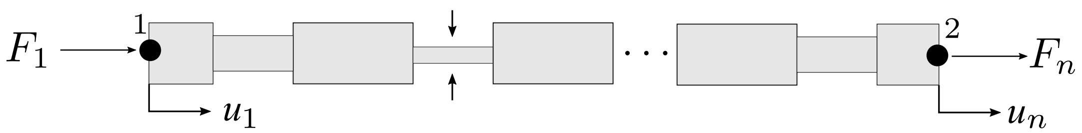

Figure 3.4: Model of damaged periodic structure with excitation and measured point.

In the Figure 3.4, the damaged periodic structure is represented. For FRAC analysis, point

1 is the position of force excitation and point 2 is the measured position.

3.1.2 Frequency response-function curvature method

The Frequency Response-Function (FRF) Curvature Method is a complete method because it detects, localizes and, predicts the damage. The change in dynamic properties (mass, stiffness, and damping) indicates the presence of damage to the structure, thus causing it more detectable in comparison methods. The FRF Curvature Method is based on The Mode Shape Curvature Method, studied by Pandey et al. (1991), however the FRF Curvature Method studies all the frequencies in the measurement range and not just the modal frequencies, as in Pandey et al. (1991) Method. So, the method consists of analyzing all frequencies, FRF data completely. This method uses the frequency response measured at different positions in the structure. For each frequency, a curvature is measured:

$$H''_{i,j} = \frac{H(\omega)_{i+1,j} - 2H(\omega)_{i,j} + H(\omega)_{i-1,j}}{h^2} \tag{3.5}$$

in which $H_{i,j}$ is the receptance FRF measured at location i for a force at location j, and h is the distance between the measurement points $i+1$ and $i-1$.

One way to find the region with damage in this type of method is to make the absolute difference, $\Delta H''_{i,j}$, between the FRF curvatures of the damaged and undamaged structure, always measured at the same point.

$$\Delta H''_{i,j} = \sum_{\omega} |H''_d(\omega)_{i,j} - H''(\omega)_{i,j}| \tag{3.6}$$

where the subscript d refers to the damaged structure.

And to finish the damage detection, the sum of the absolute difference is performed in the same case of location.

$$S_i = \sum_{j} \Delta H''_{i,j} \tag{3.7}$$

In the FRF curvature analysis, the dynamic stiffness matrix is obtained by the rearrangement of dynamic stiffness matrices. Thus, it is possible to obtain the FRF response after each cell.

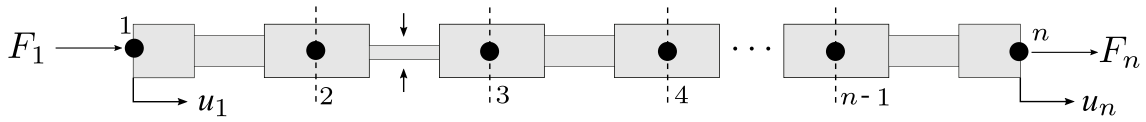

Figure 3.5: Model of damaged periodic structure with excitation and measured point.

In the Figure 3.5, the damaged periodic structure is represented. For FRF curvature analysis, point 1 is the point of force excitation. And all the following points are used in each FRF curvature analysis, as a measured points.

3.2 Chapter remarks

In this chapter, a model for structural damage was proposed, showing how it would be simulated in the analysis of periodic structures. For the identification of this damage, two metrics were chosen, Frequency Response Assurance Criterion (FRAC) and Frequency Response-Function Curvature Method, which helped to detect the damaged structure. A mathematical model was developed for these correlation methods. These methods are used in the next chapter to identify, locate and quantify the damage to the periodic structure.

Chapter 4

Analysis and results

In this chapter, numerical analysis is performed using the models presented in the previous chapter. The study was based on frequency response functions (FRFs) analysis to assess the behavior of the periodic model.

The first analysis performed aimed to understand the damage behavior in the frequency response. The damage was inserted into the periodic structure and its area was varied. The second part of the analyzes, which are the comparison methods, aimed to locate and identify the damage in the periodic model. In this second analysis, the damaged area was also modified to show its intensity. It was also studied in all analyzes, the damage interference in each position of the structure.

Therefore, the three-element cell is made of only one material, Aluminum. Both the first and third elements have the same length, L_1, this varies only with the number of cells. However, the central element varies concerning the percentage of the fixed element length, L_1. The forced response of the bar and beam was analyzed considering a free free boundary condition.

4.1 Damaged structure

In this section, numerical simulations are performed longitudinal and bending vibration on a periodic bar/beam consisting of 15 cells. The bar and beam structure has established properties. The total length, L_{total} is 1.5 m. The damaged cell has a thickness fixed at 5 mm.

4.1.1 Longitudinal response

To understand the way a damage affects a periodic structure, a variation of one hole size was analyzed in for different positions. In this first analysis, a harmonic axial force of magnitude 1 N was applied at one end of the beam and the longitudinal displacement was measured at the other end. The size of of a hole was varied considering a normal distribution with standard deviation being 20 % of the hole size. To obtain the statistical results defining the frequencies responses, the simulation was executed 1000 times.

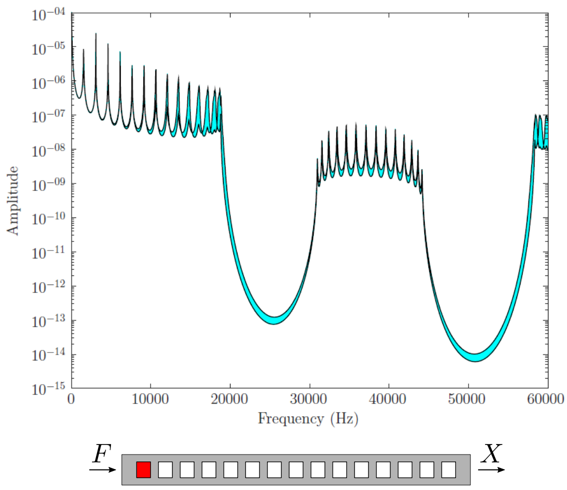

(a)

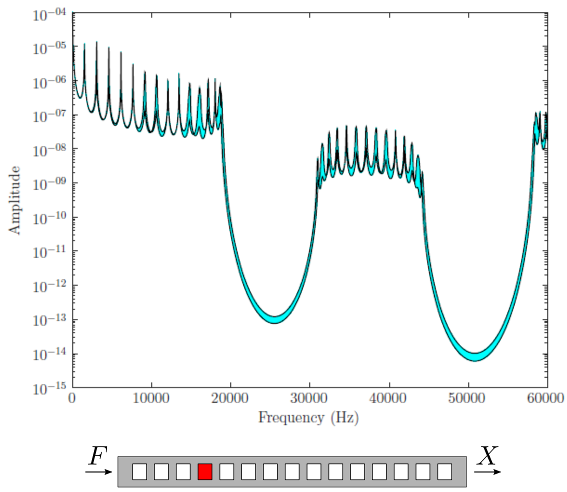

(b)

Figure 4.1: Frequency response comparison for different damage positions (Longitudinal vibration). The upper and lower curves correspond to percentile 90 and 10, respectively. From Figure (a) and(b), the damage position was in the first and fourth hole, varying with a normal distribution and standard deviation corresponding to 20% of the nominal hole area.

The results shown in Figure 4.1 illustrates the results for this analysis. Below the figures, there is a illustration showing the position of a possible damage. Figure 4.1(a) and Figure 4.2(d) with damages in the first and last cell produces very similar results, there is almost no frequency shifts in the pass band region between the two stop bands.

As the damage moves from to the middle of the bar, the pass band range is more affected by the changes in the cross section, as seen in Figure 4.1(b) and 4.2(c). Both the frequency

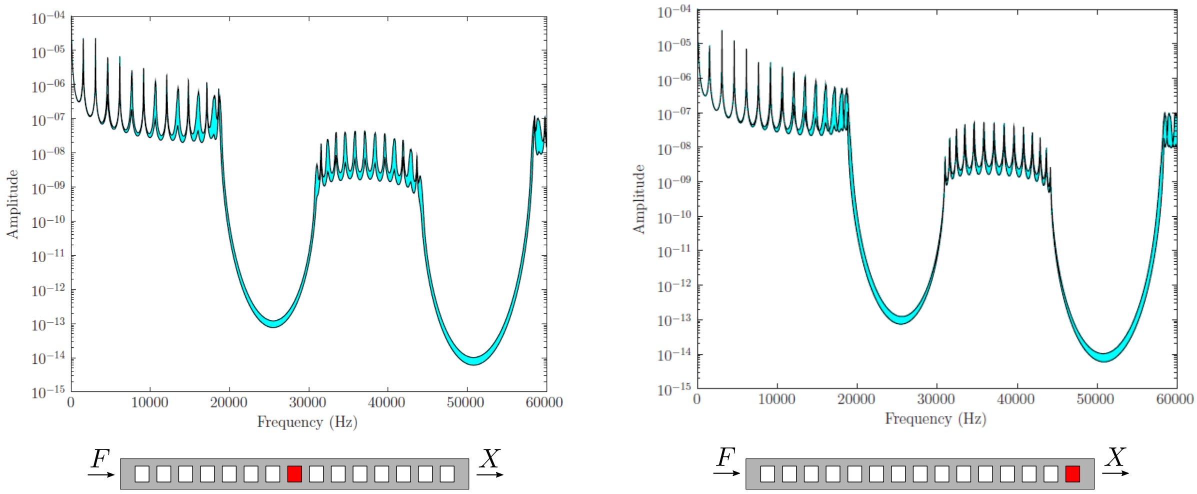

(c) (d)

Figure 4.2: Frequency response comparison for different damage positions (Longitudinal vibration). The upper and lower curves correspond to percentile 90 and 10, respectively. From Figure (c) and (d), the damage position was in the middle and last hole, varying with a normal distribution and standard deviation corresponding to 20% of the nominal hole area.

and amplitudes are affect by the change in one cell of the bar.

4.1.2 Bending response

A similar analysis based on the procedure described in the last subsection was performed for bending vibration. In this case, the results are shown in Figure 4.3. In this case, the results shown that bending vibration behaves differently from the longitudinal vibration. Changes in the first cell produce large variation in the frequency response than changes in the middle of the beam. To better observe this effect, the Figure 4.4, showing the effects on the stop band in the range 6-12 kHz.

4.2 Comparison methods

4.2.1 Frequency response function (FRF) curvature method

The first comparison method performed was the Frequency Response Function (FRF) Curvature Method, which analyzed a range of measured frequencies. The numerical simulations of

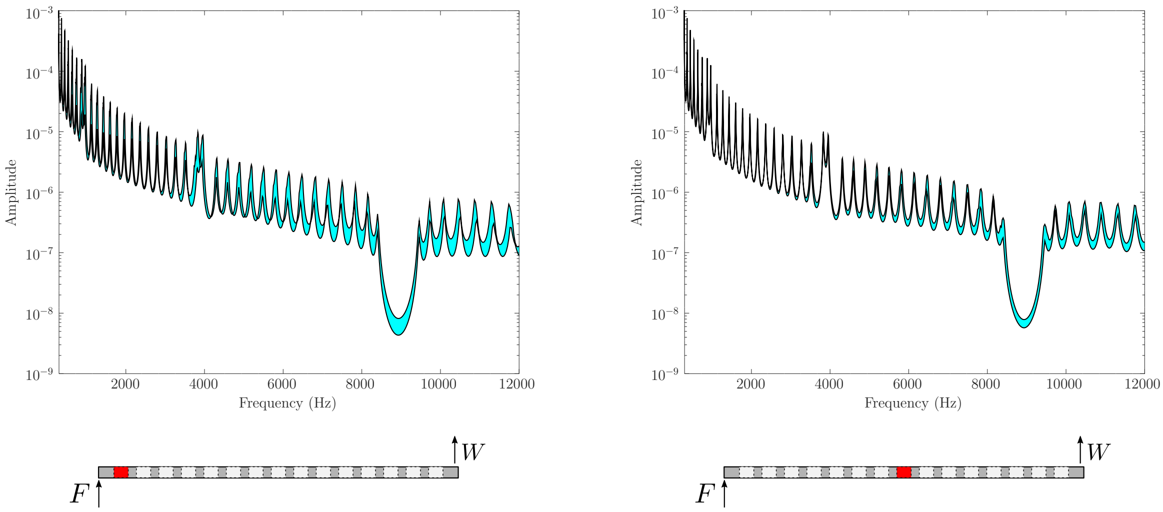

(a) (b)

Figure 4.3: Frequency response comparison for different damage positions (Bending vibration). The upper and lower curves correspond to percentile 90 and 10, respectively.

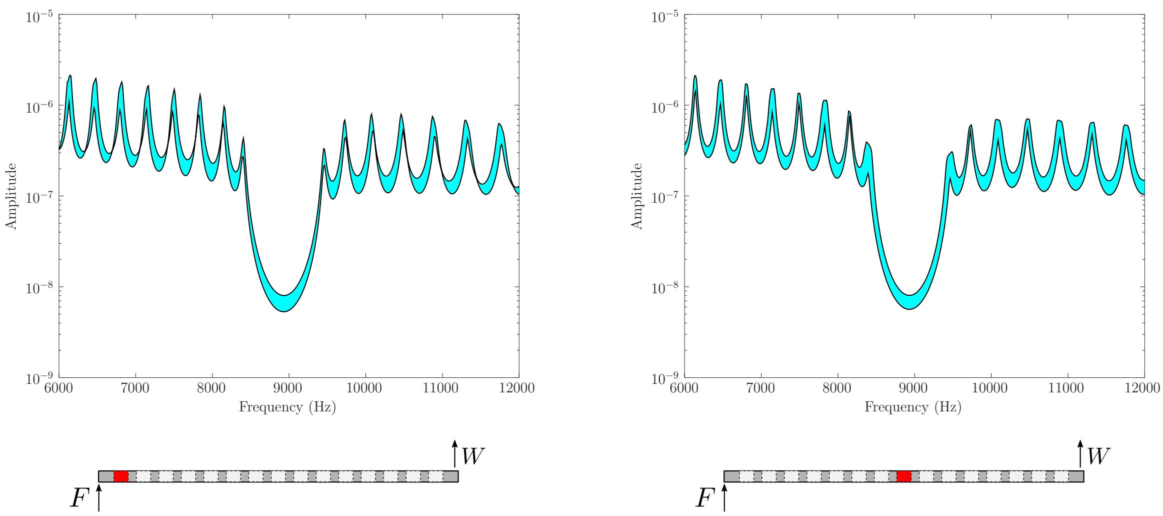

(a) (b)

Figure 4.4: Detail of frequency response comparison for different damage positions (Bending vibration). The upper and lower curves correspond to percentile 90 and 10, respectively.

this comparison method are analyzed longitudinal vibration on a periodic bar consisting of 10 cells, and total length is $1m$.

It is assumed that the position of the damage and its characteristics are not known. What makes it similar to the practical cases of vibration monitoring, where the size and location of the damage in the structure are not known. To simulate the damage, the middle part of the cell of just one cell was changed. In this middle part, its length was changed, varying this damage by 70, 75, 80, 90, 95 and 98% of the original area. And the damage was introduced between the cells analyzed in each case.

As proposed in the study of Sampaio et al. (1999), the FRF curvature method worked better for a specific frequency range, before the first anti-resonance or resonance. So, the influence of the frequency range was studied in the analyzed structure. First, the complete frequency range, 0 to 100 Hz, were analyzed for the damaged and undamaged model. The damage is located in the fifth cell. And then, the damage was detected in this frequency range for the FRF curvature method.

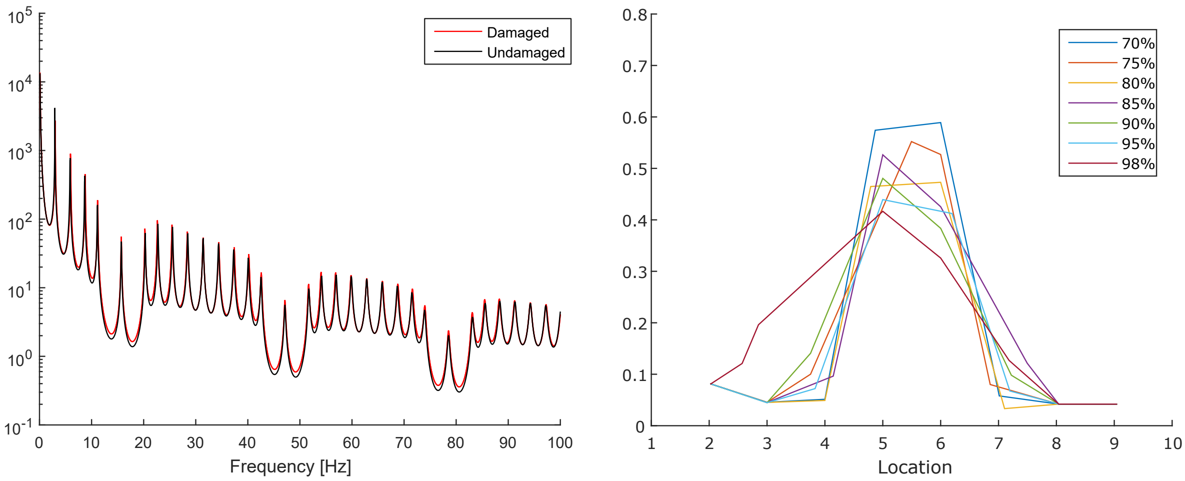

(a) (b)

Figure 4.5: (a) Receptance FRFs of the undamaged and damaged model for a frequency range of 0-100 Hz. (b) FRFs curvature differences for a frequency range of 0-100 Hz. Input force at location 1. Damage ranges from 2% to 30%, at position 5.

Analyzing the results of Figure 4.5, it's concluded that for the total frequency range, the detection of the damage location is not effective. Therefore, the frequency range has been limited to 0 - 50 Hz. And it was noticed that the FRF curvature method is more effective for this frequency range, in Figure 4.6.

Then, for all the following analyses, the frequency range from 0 to 50 Hz was established. And so, the damage in each cell position was varied so that its behavior could be studied. The damage is in the first and second cell in Figure 4.7.

Later, the damage is in the third and forth cell, Figure 4.8.

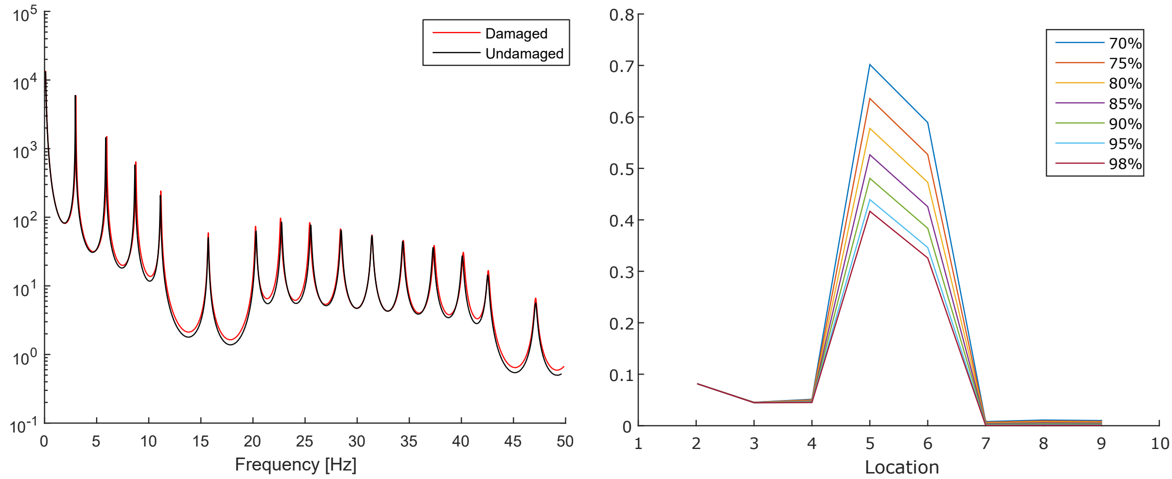

(a) (b)

Figure 4.6: (a) Receptance FRFs of the undamaged and damaged model for a frequency range of 0-50 Hz. (b) FRFs curvature differences for a frequency range of 0-50 Hz. Input force at location 1. Damage ranges from 2% to 30%, at position 5.

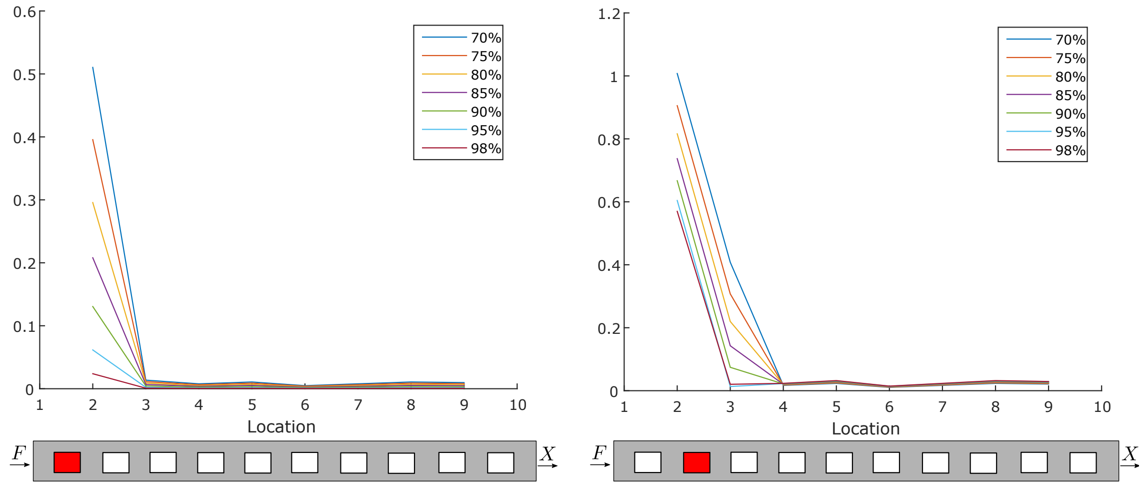

(a) (b)

Figure 4.7: FRFs curvature differences for a frequency range of 0-50 Hz. Input force at location 1. Damage ranges from 2% to 30%, at positions 1 (a) and 2 (b).

The Figure 4.9 shows the damage in the position five and six of the cell.

Follow this results, Figure 4.10 has the damage in the seven and eight position.

And finally, the damage is in the ninth and last cell, Figure 4.11.

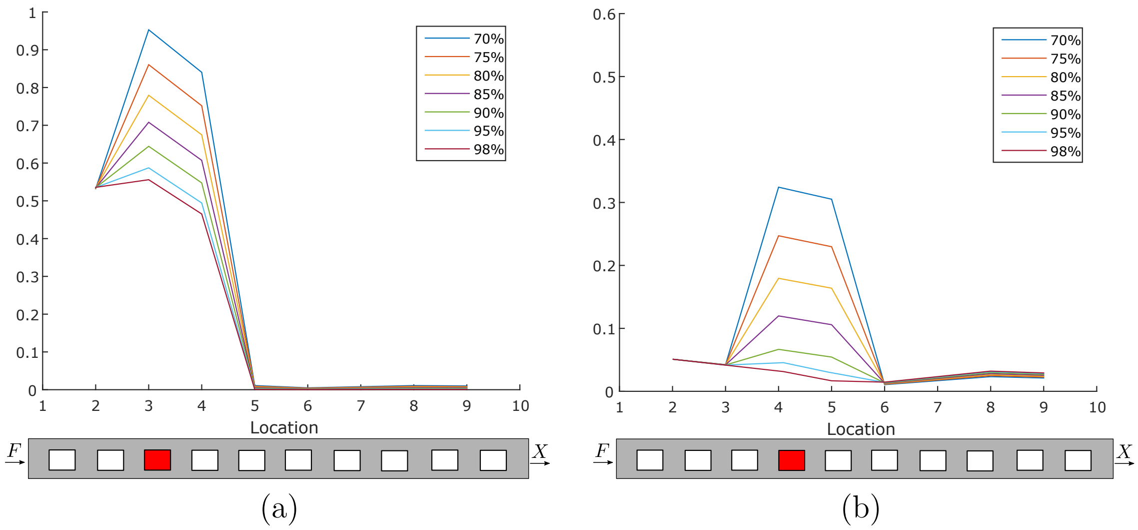

Figure 4.8: FRFs curvature differences for a frequency range of 0-50 Hz. Input force at location 1. Damage ranges from 2% to 30%, at positions 3 (a) and 4 (b).

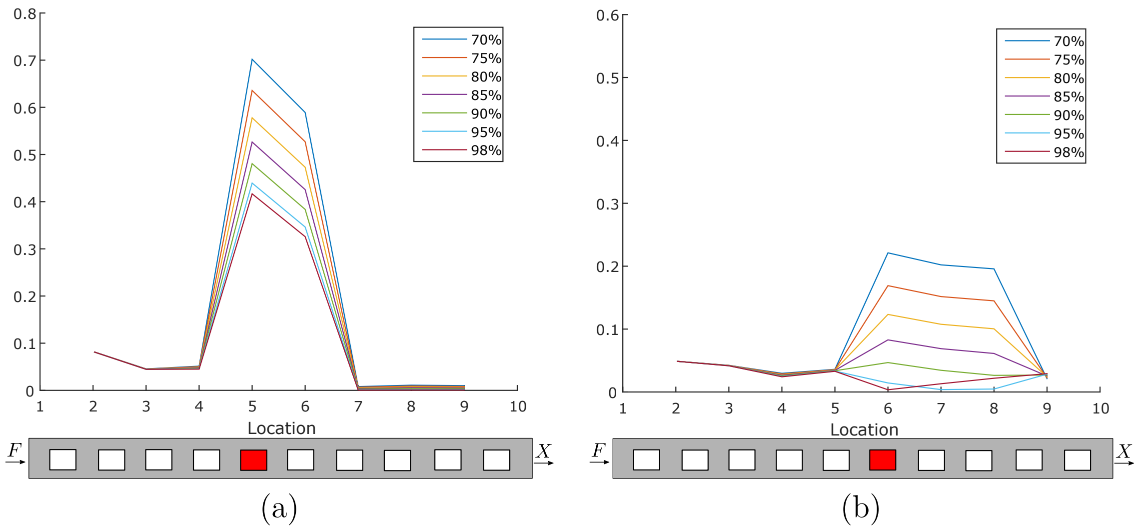

Figure 4.9: FRFs curvature differences for a frequency range of 0-50 Hz. Input force at location 1. Damage ranges from 2% to 30%, at positions 5 (a) and 6 (b).

4.2.2 Frequency response assurance criterion (FRAC)

The properties and data used for the analysis are the same as for Frequency Response Function (FRF) Curvature Method. In this analysis, the damage was simulated in different positions of the bar, Figure 4.12 e Figure 4.13. The damage was placed in the middle of the cell, varying from the first to the tenth cell of the structure. Seven levels of damage at each cell location were considered. The frequency range used is the same as the previous method, 0-50 Hz, as it

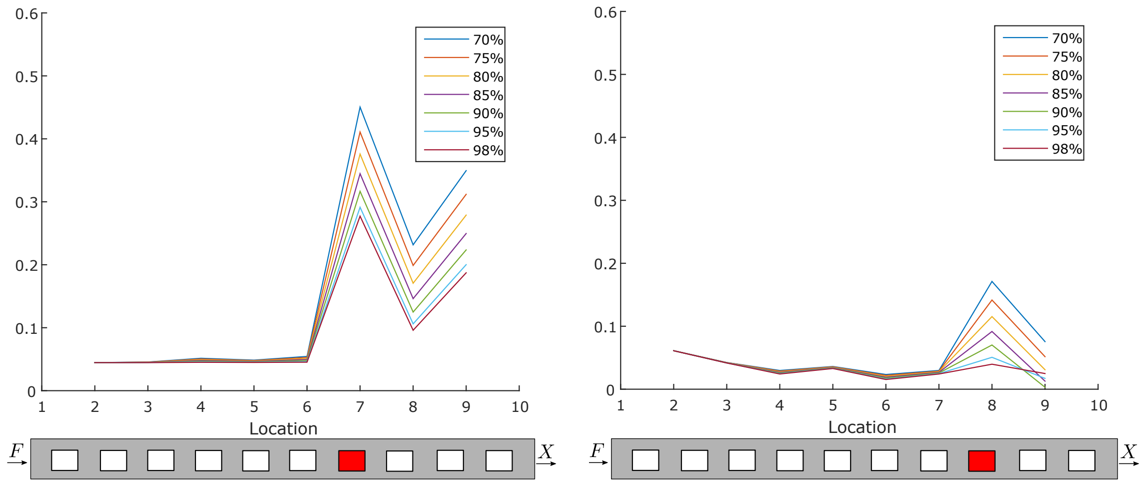

(a) (b)

Figure 4.10: FRFs curvature differences for a frequency range of 0-50 Hz. Input force at location 1. Damage ranges from 2% to 30%, at positions 7 (a) and 8 (b).

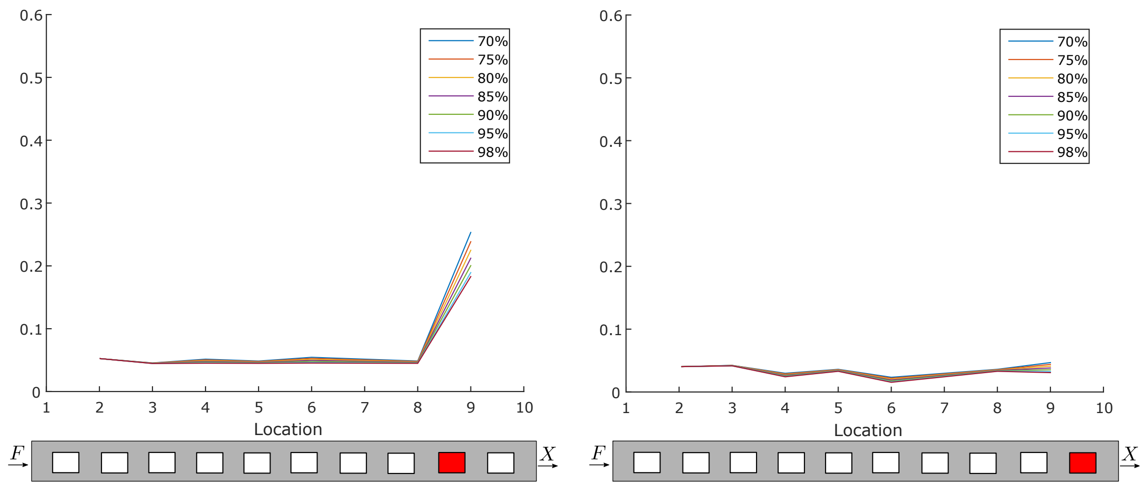

(a) (b)

Figure 4.11: FRFs curvature differences for a frequency range of 0-50 Hz. Input force at location 1. Damage ranges from 2% to 30%, at positions 9 (a) and 10 (b).

obtained better results when the frequency range is smaller.

4.2.3 Analysis of the damaged structure with 2 damages

A structure with two damages was used to validate the proposed damage identification method. It was used the Frequency response function (FRF) curvature method and Frequency response assurance criterion (FRAC), with the same characteristics used in the analysis with one damage. The numerical simulations of these comparison methods are analyzed longitudinal vibra-

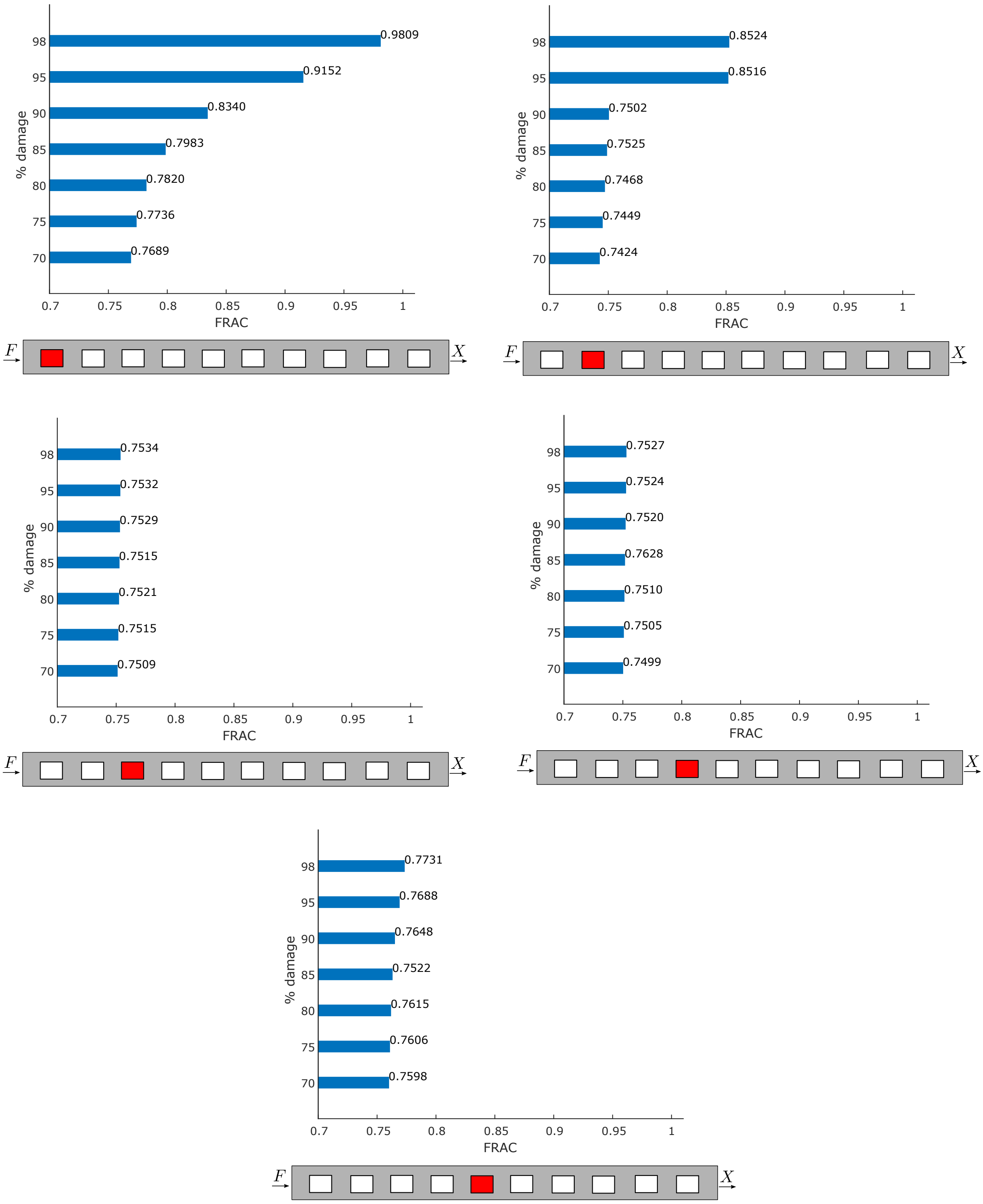

Figure 4.12: FRAC value for the damaged model, with 2% to 30% damage variation, in cell positions 1 to 5.

tion on a periodic bar consisting of 10 cells, and total length is $1m$. To simulate the damage, the middle part of the cell of just one cell was changed. In this middle part, its length was

Figure 4.13: FRAC value for the damaged model, with 2% to 30% damage variation, in cell positions 6 to 10.

changed, varying this damage by 75, 85 and 95%. And the damage was introduced between the cells analyzed in each case. The frequency range used is the same as the previous analysis, 0-50 Hz. The damage positions were chosen to understand the behavior of the structure when there are two damages in it.

- two damages at the beginning of the structure;
- one damage at the beginning and one at the end of the structure;
- two damages in the middle of the structure;
- one damage in the middle and one at the end of the structure;
- two damages at the end of the structure.

The Figure 4.14 shows the damages in the second and third position of the cell.

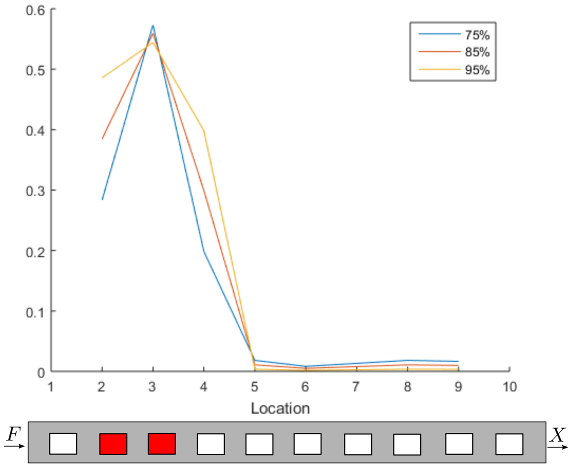

Figure 4.14: FRFs curvature differences for structure with two damages. Input force at location 1. Damage ranges from 5% to 25%, at positions 2 and 3.

Follow this results, Figure 4.15 (a) shows the damages in the second and ninth position. And Figure 4.15 (b) shows the damages in the middle of the structure, at position 4 and 5.

And finally, the damages are in the end of the structure. Figure 4.16 (a) shows damages at positions 5 and 9, and Figure 4.16 (b) damages are at positions 8 and 9.

The Figure 4.17 shows the damages in the second and third position of the cell.

Follow this results, Figure 4.18 (a) shows the damages in the second and ninth position. And Figure 4.18 (b) shows the damages in the middle of the structure, at position 4 and 5.

And finally, the damages are in the end of the structure. Figure 4.19 (a) shows damages at positions 5 and 9, and Figure 4.19 (b) damages are at positions 8 and 9.

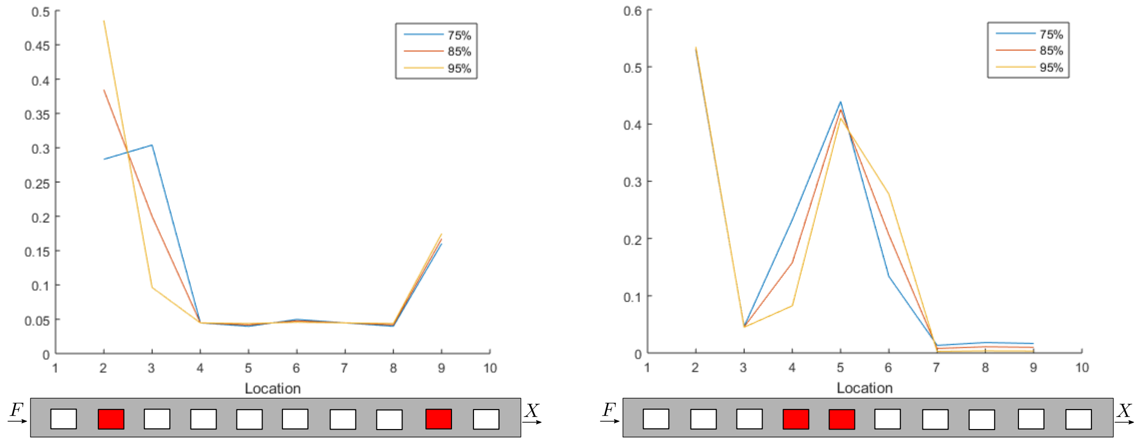

(a) (b)

Figure 4.15: FRFs curvature differences for structure with two damages. Input force at location 1. Damage ranges from 5% to 25%, at positions 2 and 9 (a) and at positions 4 and 5 (b).

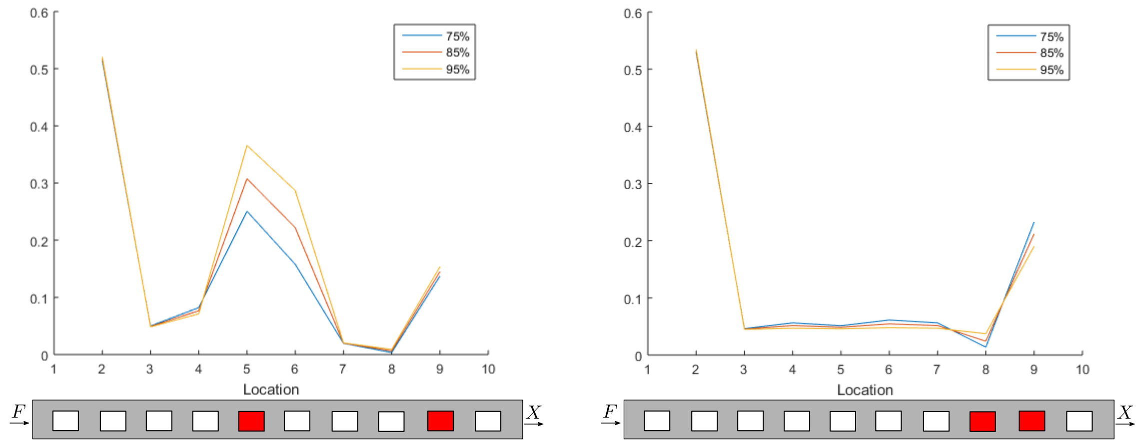

(a) (b)

Figure 4.16: FRFs curvature differences for structure with two damages. Input force at location 1. Damage ranges from 5% to 25%, at positions 5 and 9 (a) and at positions 8 and 9 (b).

4.3 Chapter remarks

In this chapter the analyzes and the results for periodic structure were presented. The first analysis showed the damage behavior in the frequency response, for longitudinal and bending vibration. Later, the damage was inserted into the periodic structure and its area was varied. And, its behaviour was interpreted. The second part, which are the comparison methods,

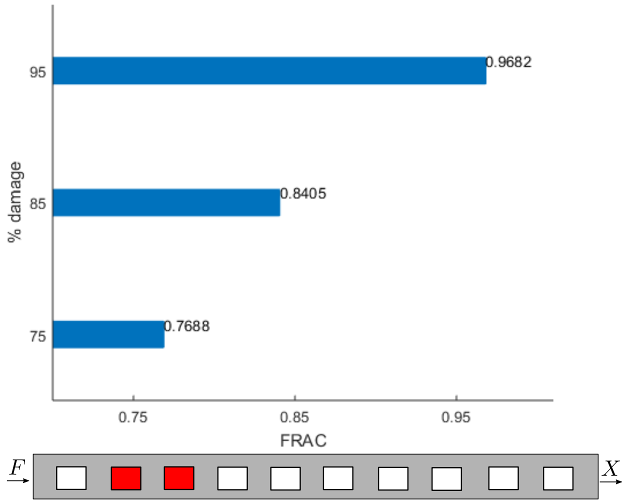

Figure 4.17: FRAC value for the damaged model with two damages, with 5% to 25% damage variation, at positions 2 and 3.

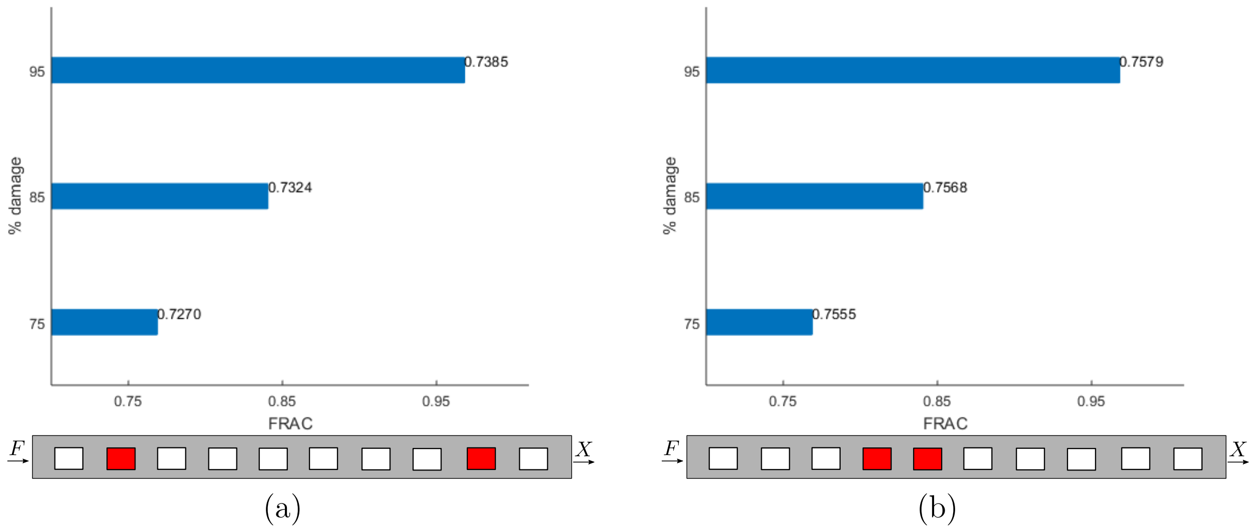

Figure 4.18: FRAC value for the damaged model with two damages, with 5% to 25% damage variation, at positions 2 and 9 (a) and at positions 4 and 5 (b).

the damaged area was also modified to show its intensity. It was also showed in all analyzes, the damage interference in each position of the structure. The final part of this analysis, a structure with two damages was analyzed to validate the identification method.

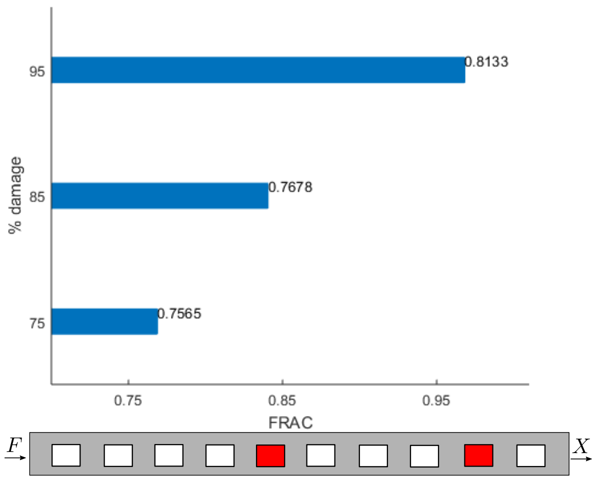

(a)

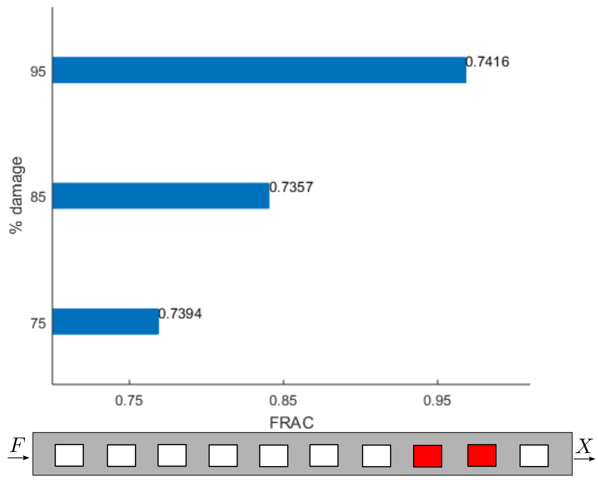

(b)

Figure 4.19: FRAC value for the damaged model with two damages, with 5% to 25% damage variation, at positions 5 and 9 (a) and at positions 8 and 9 (b).

Chapter 5

Conclusions

Structures such as bridges, aircraft, buildings, ships, are examples of structures with periodic parts, those cause accidents that could be avoided with structural health monitoring. The motivation for many studies in this area is due to the importance of economic and security aspects. The monitoring of structures has been improved, there are methods such as strain gages, visual inspection, among others, but these types of detection occur periodically. And the time between one inspection and the next can become fatal. Thus, this present research sought to detect damage continuously as an object of study to improve their identification and make their location more efficient. In this last chapter, the conclusions of the present work are discussed.

5.1 Conclusions

In the first part of this study, considering a periodic structure with 15 cells, the band gap region is formed at lower frequencies in longitudinal vibration, around 3 kHz, than in bending vibration, which has the first significant band gap near 8 kHz. In bending vibration, it is also observed that the attenuation regions increase with increasing frequency.

It is concluded that for longitudinal vibration, the position of the damage interferes when it is near the middle of the bar, showing variation in both amplitude and frequency. However, for bending vibration, the largest interference in frequency response is identified when damage changes are made in the first cell than in the middle of the beam.

The FRF curvature method is not efficient when damage is near to the end of the structure, it cannot measure damage in the first and last cell, because of its mathematical formulation. However, this method detects the presence of the damage, with better results when the damage is in the middle of the model. it is observed that the FRF curvature increases according to the damage intensity, that is, it is possible to quantify the damage. And all the results confirmed that the FRF curvature method is performed well in detecting, locating, and quantifying the damage.

The other method of correlation, FRAC, identify the presence of the damage, but not the intensity of it, the structure can be 2 or 30 % damaged that the result does not have a significant variation. However, when damage position is at the extremities, the sensitivity to its intensity is bigger than when the damage is in the middle or near to the middle.

The results with two damages in the structure for the FRF method present a mathematical flaw for damages located in the extremities, therefore it was chosen damages close to the extremities to simulate damages in the beginning and end of the structure. It is possible to identify the position the damage is in, as the peaks show the location of the damage. Increasing the FRF curve indicates that there is damage at that position. This method is most effective when damage is near the middle of the structure. However, with the presence of more damage, there was interference in the FRF curvature. It showed peaks at the beginning of the structure even though there was no damage in that position.

As seen in the structure results with damage, the Frac method identifies the damage but does not show its position. The same occurred in the analysis of the structure with two damages. This method shows that with few variations in the damaged area, the FRAC value becomes more sensitive and appears smaller than with damaged structure.

When we analyze the correlation methods, the results of both methods, FRAC and, FRF complement each other. The FRF method locates and quantifies the damage of the structure. Combining that, the FRAC method is applied to analyze the damage position in the extremities, as it is a fault of the FRF method.

5.2 Contributions

Parts of this work have been presented at the 25th International Congress of Mechanical Engineering (COBEM) as *Dynamic Analysis of Periodic Structures in beams and bars with identification of damage*

Bibliography

R.J. Allemang and D.L. Brown. A correlation coefficient for modal vector analysis. In *Proceedings of the 1st international modal analysis conference*, volume 1, pages 110–116, 1982.

S. Chesné and A. Deraemaeker. Damage localization using transmissibility functions: a critical review. *Mechanical systems and signal processing*, 38(2):569–584, 2013.

DLPNG. Traintracks png, Acess 2020-04-22. URL `https://bit.ly/2VZlnV4`.

S.W. Doebling, C.R. Farrar, M.B. Prime, et al. A summary review of vibration-based damage identification methods. *Shock and vibration digest*, 30(2):91–105, 1998.

J.F. Doyle. *Wave propagation in structures: spectral analysis using fast discrete Fourier transforms*. Springer Science & Business Media, 2012.

C.R. Farrar and K. Worden. An introduction to structural health monitoring. *Philosophical Transactions of the Royal Society of London A: Mathematical, Physical and Engineering Sciences*, 365(1851):303–315, 2007.

C.R. Farrar, G. Park, D.W. Allen, and M.D. Todd. Sensor network paradigms for structural health monitoring. *Structural control and health monitoring*, 13(1):210–225, 2006.

A. Fregolent and W. D.Ambroglo. Evaluation of different strategies in the parametric identification of dynamic models. In *ASME Conference on Mechanical Vibration and Noise*, 1997.

G.S. Gupta. Natural flexural waves and the normal modes of periodically-supported beams and plates. *Journal of Sound and Vibration*, 13(1):89–101, 1970.

W. Heylen and S. Lammens. Frac: a consistent way of comparing frequency response functions. In *Proceedings of the conference on identification in engineering systems*, pages 48–57, 1996.

D.J. Inman, C.R. Farrar, V.L. Junior, and V.S. Junior. *Damage prognosis: for aerospace, civil and mechanical systems.* John Wiley & Sons, 2005.

R.D. Kangwai and S.D. Guest. Symmetry-adapted equilibrium matrices. *International Journal of Solids and Structures*, 37(11):1525–1548, 2000.

R.D. Kangwai, S.D. Guest, and S. Pellegrino. An introduction to the analysis of symmetric structures. *Computers & structures*, 71(6):671–688, 1999.

M. Kimsan et al. Sensitivity of frfs curvature difference method in detecting damage. *International Journal of Theoretical and Applied Mechanics*, 1:185–187, 1998.

G.J. Kissel. Localization factor for multichannel disordered systems. *Physical Review A*, 44 (2):1008, 1991.

R.S. Langley. On the forced response of one-dimensional periodic structures: Vibration localization by damping. *Journal of Sound and Vibration*, 178(3):411–428, 1994.

U. Lee. *Spectral element method in structural dynamics.* John Wiley & Sons Inc, 2009.

U. Lee and J. Shin. A frequency response function-based structural damage identification method. *Computers & Structures*, 80(2):117–132, 2002.

X.Q. Liang, Q. Gao, and W.A. Yao. An efficient algorithm based on group theory and the woodbury formula for the dynamic responses of periodic structures. *Computers & Structures*, 182:238–251, 2017.

T. Marwala and P.S. Heyns. Multiple-criterion method for determining structural damage. *Aiaa Journal*, 36(8):1494–1501, 1998.

D.J. Mead. Wave propagation and natural modes in periodic systems: Ii. multi-coupled systems, with and without damping. *Journal of Sound and Vibration*, 40(1):19–39, 1975.

D.J. Mead. Wave propagation in continuous periodic structures: research contributions from southampton, 1964–1995. *Journal of sound and vibration*, 190(3):495–524, 1996.

D.J. Mead. *Passive vibration control.* John Wiley & Sons Inc, 1999.

A. Mohammadirad, A.A.S. Akmal, and R. Vakili. Improvement of partial discharge localization accuracy using frequency response assurance criterion. *Power System Conference*, 2018.

D.J. Nefske and S.H. Sung. Correlation of a coarse-mesh finite element model using structural system identification and a frequency response assurance criterion. In *International Society for Optical Engineering.* International Society for Optical, 1996.

N. Olhoff, B. Niu, and G. Cheng. Optimum design of band-gap beam structures. *International Journal of Solids and Structures*, 49(22):3158–3169, 2012.

W.M. Ostachowicz. Damage detection of structures using spectral finite element method. *Computers & structures*, 86(3-5):454–462, 2008.

A.K. Pandey, M. Biswas, and M.M. Samman. Damage detection from changes in curvature mode shapes. *Journal of sound and vibration*, 145(2):321–332, 1991.

D.M. Reddy and S. Swarnamani. Application of the frf curvature energy damage detection method to plate like structures. *World Journal of Modelling and Simulation*, 8(2):147–153, 2012.

S. Rubin. Mechanical immittance-and transmission-matrix concepts. *The Journal of the Acoustical Society of America*, 41(5):1171–1179, 1967.

R.P.C. Sampaio, N.M.M. Maia, and J.M.M. Silva. Damage detection using the frequency-response-function curvature method. *Journal of sound and vibration*, 226(5):1029–1042, 1999.

Scientific Diagram. An aircraft fuselage png, Acess 2020-04-22a. URL `https://bit.ly/2xV6T0z`.

Scientific Diagram. Satellite png, Acess 2020-04-22b. URL `https://bit.ly/3eQ9OrQ`.

E. Tassilly. Propagation of bending waves in a periodic beam. *International journal of engineering science*, 25(1):85–94, 1987.

E.E. Ungar. Steady-state responses of one-dimensional periodic flexural systems. *The Journal of the Acoustical Society of America*, 39(5A):887–894, 1966.

Z. Wanxie and Q. Chunhang. Analysis of symmetric or partially symmetric structures. *Computer Methods in Applied Mechanics and Engineering*, 38(1):1–18, 1983.

HJ. Xiang and ZF. Shi. Analysis of flexural vibration band gaps in periodic beams using differential quadrature method. *Computers & structures*, 87(23-24):1559–1566, 2009.